
Interpreting Neural Networks through the Polytope Lens

Sid Black* Lee Sharkey* Leo Grinsztajn Eric Winsor Dan Braun

Jacob Merizian Kip Parker Carlos Ramón Guevara Beren Millidge

Gabriel Alfour

Connor Leahy

Abstract

Mechanistic interpretability aims to explain what a neural network has learned at a nuts-and-bolts level. What are the fundamental primitives of neural network representations? What basic objects should we use to describe the operation of neural networks mechanistically? Previous mechanistic descriptions have used individual neurons or their linear combinations to understand the representations a network has learned. But there are clues that neurons and their linear combinations are not the correct fundamental units of description—directions cannot describe how neural networks use nonlinearities to structure their representations. Moreover, many instances of individual neurons and their combinations are polysemantic (i.e. they have multiple unrelated meanings). Polysemanticity makes interpreting the network in terms of neurons or directions challenging since we can no longer assign a specific feature to a neural unit. In order to find a basic unit of description that doesn't suffer from these problems, we zoom in beyond just directions to study the way that piecewise linear activation functions (such as ReLU) partition the activation space into numerous discrete polytopes. We call this perspective the ‘polytope lens’. Although this view introduces new challenges, we think they are surmountable and that more careful consideration of the impact of nonlinearities is necessary in order to build better high-level abstractions for a mechanistic understanding of neural networks. The polytope lens makes concrete predictions about the behavior of neural networks, which we evaluate through experiments on both convolutional image classifiers and language models. Specifically, we show that polytopes can be used to identify monosemantic regions of activation space (while directions are not in general monosemantic) and that the density of polytope boundaries reflect semantic boundaries. We also outline a vision for what mechanistic interpretability might look like through the polytope lens.

*equal contribution

Contents

1	Introduction	2
1.1	Are individual neurons the fundamental unit of neural networks?	3
1.2	Are directions the fundamental unit of neural networks?	3
2	The Polytope Lens	6
2.1	Polytopes as the atoms of neural networks & polytope regions as their molecules . . .	9
2.1.1	Prediction 1: Polysemantic directions overlap with multiple monosemantic polytope regions	10
2.1.2	Prediction 2: Polytope boundaries reflect semantic boundaries	13
2.1.3	Prediction 3: Polytopes define when feature-directions are on- and off-distribution	17
3	Discussion	18
4	Related work	21
4.1	Interpreting polytopes, single neurons, or directions	21
4.2	Polysemanticity and Superposition	21
A	Polytope density while interpolating between activations caused by images	26
B	Scaling activation vectors and plotting polytope density	28
C	Mathematical account of neural networks as max affine spline operators (MA-SOs)	29
D	Note on Terminology of Superposition, Interference, and Aliasing	30
E	Examples of Text Clusters from GPT2-Small	31

1 Introduction

How should we carve a neural network at the joints? Traditionally, mechanistic descriptions of neural circuits have been posed in terms of neurons, or linear combinations of neurons also known as ‘directions’. Describing networks in terms of these neurons and directions has let us understand a surprising amount about what they’ve learned (Cammarata et al., 2020a). But these descriptions often possess undesirable properties - such as polysemanticity and inability to account for nonlinearity - which suggest to us that they don’t always carve a network at its joints.

If not neurons or directions, then what should be the fundamental unit of a mechanistic description of what a neural network has learned? Ideally, we would want a description in terms of some object that throws away unnecessary details about the internal structure of a neural network while simultaneously retaining what’s important. In other words, we’d like a less ‘leaky’ abstraction for describing a neural network’s mechanisms.

We propose that a particular kind of mathematical object – a ‘polytope’ – might serve us well in mechanistic descriptions of neural networks with piecewise-linear activations.¹ We

¹And, with some relaxations to ‘soft’ polytopes, the polytope lens might also let us mechanistically describe neural networks with activations such as GELU and Swish. Some prior work exists that extends the polytope lens to such activations (Balestriero and Baraniuk, 2018b). See the Appendix C for further discussion.

believe they might let us build less leaky abstractions than individual neurons and directions alone, while still permitting mechanistic understandings of neural networks of comparable length and complexity.

To help explain how the polytope lens could underlie mechanistic descriptions of neural networks, we first look at the problems that arise when using individual neurons (both biological and artificial) and then when using directions as the basic units of description and suggest how this perspective offers a potential solution.

1.1 Are individual neurons the fundamental unit of neural networks?

Studying the function of single neurons has a long history. The dominant view in neuroscience for approximately one hundred years was the ‘neuron doctrine’ (Yuste, 2015). The neuron doctrine contended that the way to understand neural networks is to understand the responses of individual neurons and their role in larger neural circuits. This led to significant successes in the study of biological neural circuits, most famously in the visual system. Early and important discoveries within this paradigm included cells in the frog retina that detect small patches of motion (fly detectors) (Lettvin et al., 1959); cells in the visual cortex with small receptive fields that detect edges (Hubel and Wiesel, 1962), cells in the higher visual system that detect objects as complex as faces (Sergent et al., 1992), and many even highly abstract multimodal concepts appear to be represented in single neurons (Quian Quiroga et al., 2005, 2009).

Given their historic usefulness in the study of *biological* neural networks, individual neurons are a natural first place to start when interpreting *artificial* neural networks. Such an approach has led to significant progress. Many studies have suggested that it is possible to identify single neurons that responded to single features (Szegedy et al., 2014; Zhou et al., 2015; Bau et al., 2017; Olah et al., 2017). Analysis of small neural circuits has also been done by inspecting individual neurons (Cammarata et al., 2020c; Goh et al., 2021).

Mathematically, it’s not immediately obvious why individual neurons would learn to represent individual features given that, at least in linear networks, the weights and activations can be represented in any desired basis. One suggestion for why this would happen is the ‘privileged basis’ hypothesis (Elhage et al., 2021, 2022). This hypothesis states that element-wise nonlinear activation functions encourage functionally independent input features to align with individual neurons rather than directions.

Despite both historical success and the privileged basis hypothesis, it turns out that in many circumstances networks learn features that don’t perfectly align with individual neurons. Instead, there have been some suggestions that networks learn to align their represented features with directions (Olah et al., 2018; Saxena and Cunningham, 2019a).

1.2 Are directions the fundamental unit of neural networks?

One of the main reasons to prefer directions over individual neurons as the functional unit of neural networks is that neurons often appear to respond to multiple, seemingly unrelated things. This phenomenon is called polysemanticity.² Nguyen et al. (2016) (supplement) and Olah et al. (2017) were perhaps the first to explicitly identify neurons that represent multiple unrelated features in convolutional image classifiers. Polysemantic neurons have also been found in large language models (Geva et al., 2021) and multimodal networks (Goh et al., 2021), and in the brain (Tanabe, 2013). They are usually found by looking at the dataset examples that maximally activate specific neurons and noticing that there are multiple distinct groups of features represented in the examples. Below are a few examples of polysemantic neurons from a convolutional image classifier (InceptionV1³) and a large language model, GPT2-Medium.

²In neuroscience, the polysemanticity is called mixed selectivity (Fusi et al., 2016)

³We chose InceptionV1 since it has served as a kind of ‘model system’ in previous mechanistic interpretability work. But the Pytorch implementation of the InceptionV1 architecture (also known as GoogLeNet), it transpires, differs from the original. The original had no batch norm, whereas the Pytorch version does.

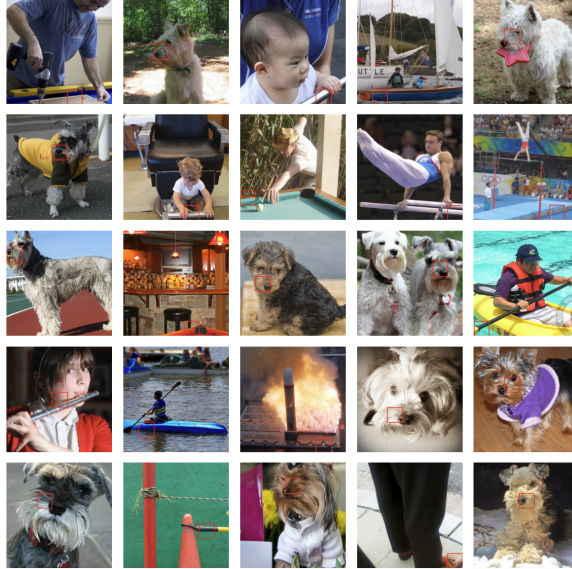


Figure 1: An example of a polysemantic neuron in InceptionV1 (layer inception5a, neuron 233) which seems to respond to a mix of dog noses and metal poles (and maybe boats).

layer-18_neuron-646

broadcast from Southern California's Indie 103 studios, but since the summer of 2010 has been broadcast as part of the Earwolf comedy podcasting network, being recorded in studios owned by the company. Many notable people in the world of comedy, music, television and film have appeared on the podcast, including Paul F. Tompkins, Lauren Lapkus, Jason Mantzoukas, "Weird Al" Yankovic, Aimee Mann, Jon Hamm, Aziz Ansari, Adam Scott, Patton Oswalt, Seth Rogen, Thomas Lennon, Zach Galifianakis, Ben Stiller, David Cross, Bob Odenkirk, Si Vincent, Sarah Silverman, Amy Poehler, James Adomian, Harris Wittels, Michael Cera, Tim Heidecker, Nick Kroll, Loudon Wainwright III, Matt Besser, Kevin Nealon, and Andy Daly. Comedy Bang! Bang! was also a television series

to be a small part of it. It was not false modesty. At \$180 a pop, the sponsorships were a bargain, considering what they offered Sam in return: a chance to be the ideal father, generous, attentive, loving, and free of all the inconsistencies and shortcomings that scarred his relationships with his own children. In 1963 the awards for High Country finally began rolling in, and the Hollywood power brokers at last took notice of the young director. Jerry Bresler—a balding, pear-shaped man in his early fifties—had produced a series of predictable action vehicles (The Vikings), tired soap operas (Diamond Head, starring Charlton Heston), and lame comedies (Gidget Goes Hawaiian and Gidget Goes to Rome). In 1963 he landed a multipicture deal with Columbia Pictures. Heston and Bresler enjoyed an an

cardiomyopathy (HCM) had intact sympathetic innervation of the hypertrophic myocardium. Clinical neurochemical studies linked specific catecholaminergic phenotypes with genotypic abnormalities in Menkes' disease, familial dysautonomia (FD), and L-aromatic-amino-acid decarboxylase (LAAAD) deficiency. Treatment with L-DOPA as a dopaminergic pro-drug produced beneficial natriuretic responses in patients with congestive heart failure. Plasma DA-sulfate levels were found to depend on dietary factors and on production of endogenous DA in the gastrointestinal tract.

auric Air Auric Air Services Limited is a small privately-owned airline based in Tanzania, Operating from Mwalimu Julius Nyerere International Airport (JNIA) Dar-es-salaam, Arusha Airport and Mwanza Airport. The Company offers scheduled flights to 42 Destinations within East Africa as

terminal DNA-binding domain and the transactivation domain of the E2 protein are involved in the interaction. By transient cotransfection assays on C-33 A cells, we demonstrated that TAF1 enhances the activation of an E2-dependent artificial promoter while overexpression of TAF1 alleviates the E2-dependent repression of a high-risk HPV long control region. The specific modification of the transcriptional activity of both promoters by TAF1 suggests that the interaction between these proteins could participate in the modulation of the transregulatory properties of E2, with important biological consequences.

Kathleen DENSBERGER, Individually and as Executrix of the Estate of Colonel William Densberger, Mary Ann Kelly, Individually and as Executrix of the Estate of Colonel Robert Kelly, Lisa Rhodes Truluck, Individually and as Executrix of the Estate of Specialist Gary Rhodes, Jr., Deborah L.

Figure 2: An example of a polysemantic neuron in GPT2-Medium. The text highlights represent the activation magnitude - the redder the text, the larger the activation. We can see that this neuron seems to react strongly to commas in lists, but also to diminutive adjectives ('small', 'lame', 'tired') and some prepositions ('of', 'in', 'by'), among other features.

One explanation for polysemantic neurons is that networks spread the representation of features out over multiple neurons. By using dimensionality reduction methods, it's often possible to find directions (linear combinations of neurons) that encode single features, adding credence to the idea that directions are the functional unit of neural networks (Olah et al., 2018; Saxena and Cunningham, 2019b; Mante et al., 2013). This chimes with the 'features-as-directions perspective' (Elhage et al., 2022). Under this perspective, the magnitude of neural activations loosely encodes 'intensity' or 'uncertainty' or 'strength of representation', whereas the direction encodes the semantic aspects of the representation.⁴

⁴Similar encoding methods have been widely observed in neuroscience where they are called "population coding". Population codes have been found or hypothesized to exist in many neural regions and especially the motor cortex.

If there are fewer features than neurons (or an equal number of both), then each feature can be encoded by one orthogonal direction. To decode, we could simply determine which linear combination of neurons encodes each feature. However, if there are more features than neurons, then features must be encoded in non-orthogonal directions and can interfere with (or [alias](#) - see Appendix D) one another. In this case, the features are sometimes said to be represented in ‘superposition’ ([Elhage et al., 2022](#)).⁵ In superposition, networks encode more features than they have orthogonal basis vectors. This introduces a problem for a naive version of the features-as-directions hypothesis: Necessarily, some feature directions will be polysemantic! If we assume that representations are purely linear, then it’s hard to see how networks could represent features in non-orthogonal directions without interference degrading their performance. Neural networks use nonlinearities to handle this issue. [Elhage et al. \(2022\)](#) argue that a Rectified Linear Unit (ReLU) activation does this through thresholding: If the interference terms are small enough not to exceed the activation threshold, then interference is ‘silenced’! For example, suppose neuron A is polysemantic and represents a cat ear, a car wheel, and a clock face, and neuron B represents a dog nose, a dumbbell, and a car wheel. When neuron A and B activate together, they can cause a downstream car neuron to activate without activating neurons that represent any of their other meanings, so long as their pre-activations are below threshold.

Beyond enabling polysemanticity, nonlinearities introduce a second problem for the features-as-directions viewpoint. The directions in each layer, caused by a direction in an earlier layer, are no longer invariant to scaling, as we would expect in a fully linear network. If we scale the activations in a particular layer in a fully linear network by some scalar multiple, we expect the class prediction to remain the same - as this is equivalent to scaling the output logits. However, if we scale the activations in a particular layer in a *non*-linear network, some neurons in later layers may ‘activate’ or ‘deactivate’. (i.e. their preactivation goes above or below threshold). In other words, scaling directions in one layer can change the direction (and hence the features represented) in later layers!

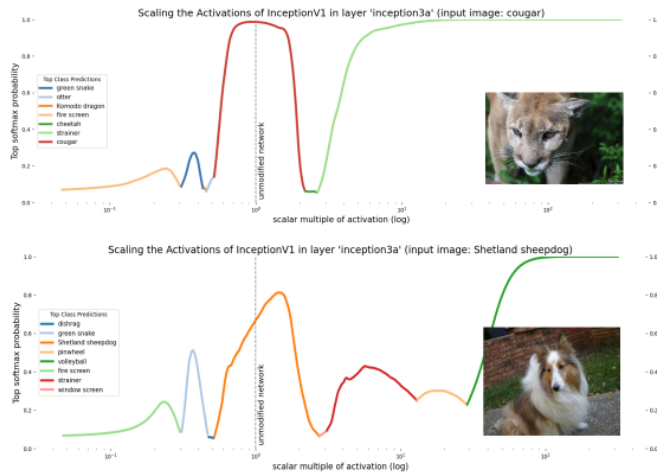


Figure 3: Scaling the activations in a layer causes semantic changes later in the network despite no change in activation direction in the scaled layer. The image on the right represents the input image.

On the one hand, we should expect scaling the activation to change the direction in later layers. On the other, this poses a challenge to the features-as-directions view; scaling all representations relative to each other shouldn’t change their meaning except by changing

⁵The idea that non-orthogonal representations interfere with each other has a long history in machine learning, starting with the study of the memory capacity of associative memories such as Hopfield networks which face the same underlying tradeoff between information capacity and orthogonality ([Hopfield, 1982](#); [Abu-Mostafa and St. Jacques, 1985](#)). When features are encoded in non-orthogonal directions, the activation of one feature coactivates all feature directions sharing a non-zero dot product with it, leading to interference.

their ‘intensity’. The naive version of the features-as-directions hypothesis requires the addition of something like a ‘distribution of validity’ within which directions represent the correct feature and outside of which they don’t. Unfortunately, the features-as-directions view doesn’t tell us what this distribution is. We’d like to know what the distribution is in order to know when our models might exhibit unpredictable out-of-distribution behavior.

Despite these two limitations (polysemanticity and failure to be invariant to scale), the features-as-directions view has enabled much progress in understanding circuits of some neural networks, even permitting [Cammarata et al. \(2021\)](#) to reverse engineer some circuits and reconstruct them by hand. So the view represents at least a substantial piece of the interpretability puzzle - and it seems true that *some* directions carry a clear semantic meaning. Another reason to believe that the features-as-directions viewpoint is sensible is that, as we scale the hidden activations, neighbouring categories are quite often (but not always) semantically related. For instance, when we scale up the hidden layer activations for the cougar image, the network misclassifies it as a cheetah, which is still a big cat!

Instead of radically overhauling the features-as-directions view, perhaps it only needs some modifications to account for the effects of nonlinearities, namely:

- Invariances - We have shown that directions are not invariant to scaling. We want a modification that captures invariances in neural networks. For instance, we want something that points the way to ‘semantic invariances’ by identifying monosemantic components of neural networks even when subjected to certain geometric transformations (like scaling).
- On/off-distribution - The features-as-directions view appears to be correct only when the scale of activations is within some permitted distribution. We want a way to talk about when activations are off-distribution with more clarity, which will hopefully let us identify regions of activation space where the behavior of our models becomes less predictable.

To find an object that meets our needs, we turn to some recent developments in deep learning theory - a set of ideas that we call the ‘polytope lens’.

2 The Polytope Lens

Let’s consider an MLP-only network which uses piecewise linear activation functions, such as ReLU.⁶ In the first layer, each neuron partitions the input data space in two with a single hyperplane: On one side, the neuron is “on” (activated) and on the other side it’s “off”.

On one side of the boundary, the input vector is multiplied by the weights for that neuron, which is just that neuron’s row of the weight matrix. On the other side, the input is instead projected to 0, as though that row of weight matrix were set to zero. We can therefore view the layer as implementing a different affine transformation on either side of the partition. For a mathematical description, see Appendix C.

The orientation of the plane defining the partition is defined by the row of the weight matrix and the height of the plane is defined by the neuron’s bias term. The example we illustrate here is for a 2-dimensional input space, but of course neural networks typically have inputs that are much higher dimensional.

Considering all N neurons in layer 1 together, the input space is partitioned N times into a number of convex shapes called polytopes (which may be unbounded on some sides). Each polytope has a different affine transformation according to whether each neuron is above or below its activation threshold. This means we can entirely replace this layer by a set of affine transformations, one for each polytope.

As we add layers on top of layer 1, we add more neurons and, thus, more ways to partition the input space into polytopes, each with their own affine transformation. Thus, neural

⁶The arguments we make in support of the Polytope Lens also apply to other activation functions such as GELU. But for simplicity we stick to piecewise linear activation functions because it’s easier to think geometrically in terms of straight lines rather than curvy ones.

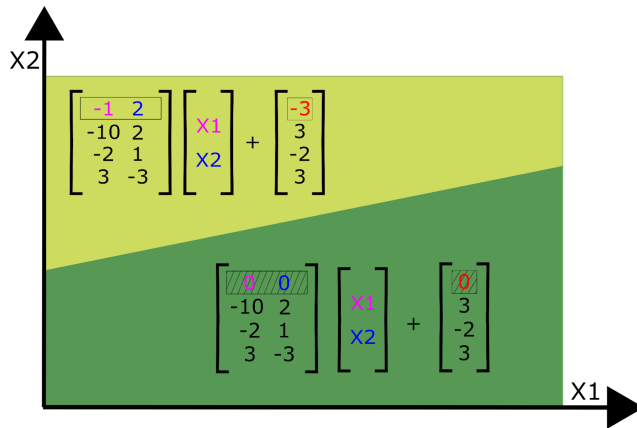


Figure 4: Affine transformations in the activated / unactivated regions of one neuron (assuming the three other neurons are activated).

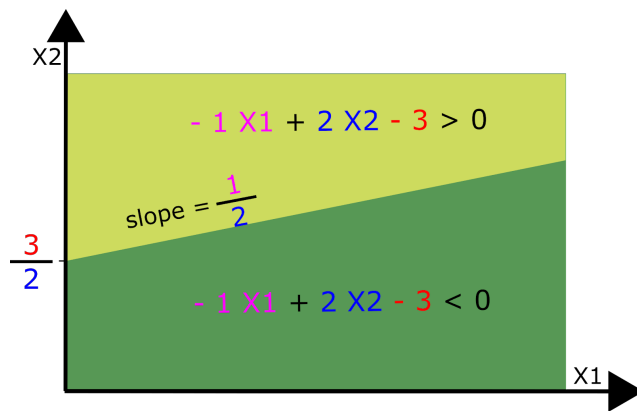


Figure 5: Polytope boundaries are defined by the weights and bias of a neuron. The weights determine the orientation of the (hyper-) plane and the bias determines its height.

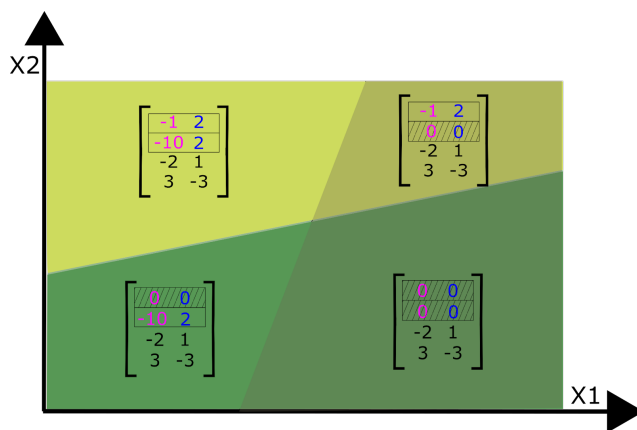


Figure 6: Four polytopes corresponding to four different affine transformations defined by two neurons in layer 1.

networks cut up the network's input space into regions (polytopes) that each get transformed by a different set of affine transformations. Adding subsequent layers permits partition boundaries that *bend* when they intersect with the partition boundaries of earlier layers (Hanin and Rolnick, 2019b). The boundaries bend in different ways depending on the weights of the neurons in later layers that activate or deactivate.

Each polytope can thus be analyzed as a fully linear subnetwork composed of a single affine transformation. Within each of these subnetworks, we would expect to see a set of interpretable directions that are scale invariant within each polytope. But the same directions in a different subnetwork might yield different interpretations. However, we should expect nearby polytope regions (subnetworks) to share similar affine transformations, and therefore similar semantics. We'll discuss this further in the next section.

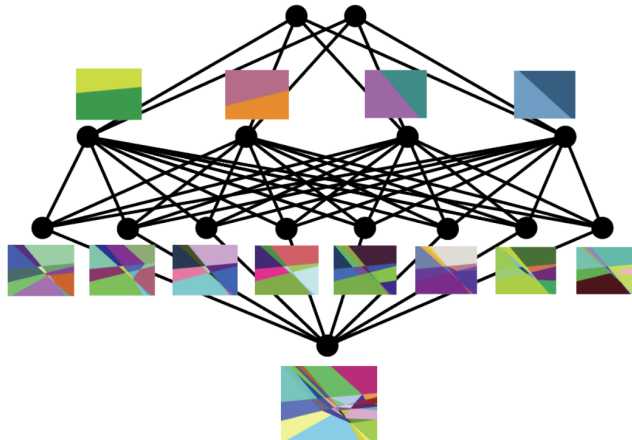


Figure 7: Image from Hanin and Rolnick (2019a)

The polytope lens draws on some recent work in deep learning theory, which views neural networks as **max-affine spline operators** (MASOs) (Balestrierio and baraniuk, 2018). For a mathematical description of the above perspective, see Appendix C.

The picture painted above is, of course, a simplified model of a far higher dimensional reality. When we add more neurons, we get a lot more hyperplanes and, correspondingly, a lot more polytopes! Here is a two dimensional slice of the polytopes in the 40768-dimensional input space of inception5a, with boundaries defined by all the subsequent layers:

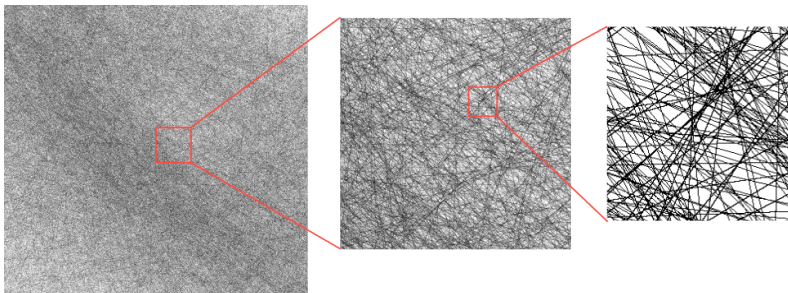


Figure 8: This figure depicts the polytope boundaries that intersect with a two-dimensional slice through the $832 * 7 * 7 = 40768$ -dimensional input space of InceptionV1 layer inception5a. The slice was defined using the activation vectors caused by three images, one of a banana, a coffee cup, and a projector. The boundaries are defined using all neurons from inception5a to the classification logits. There are many polytopes in high dimensional space. If we instead used a lower layer, e.g. inception3a, then there would be many, many more polytope boundaries.

In fact, as we add neurons, the number of polytopes the input space is partitioned into grows exponentially.⁷ Such large numbers of polytopes become quite hard to talk about! Fortunately, each polytope can be given a unique code, which we call a ‘**spline code**’, defined in the following way: Consider the sequence of layers from L to $L + K$. These layers define a set of polytope boundaries in the input space to layer L . A polytope’s spline code is simply a binary vector of length M (where M is the total number of neurons in layers L

⁷Although exponential, it’s not as many as one would naively expect - see Hanin and Rolnick (2019b).

to $L + K$) with a 1 where the polytope causes a neuron to activate above threshold and 0 otherwise. Notice that we can define a code for any sequence of layers; if we define a spline code from layer L to $L + K$, the codes correspond to the polytopes that partition layer L 's input space. There is therefore a duality to spline codes: Not only are they a name for the region of input activation space contained within each polytope, but they can also be viewed as labels for pathways through layers L to $L + K$.

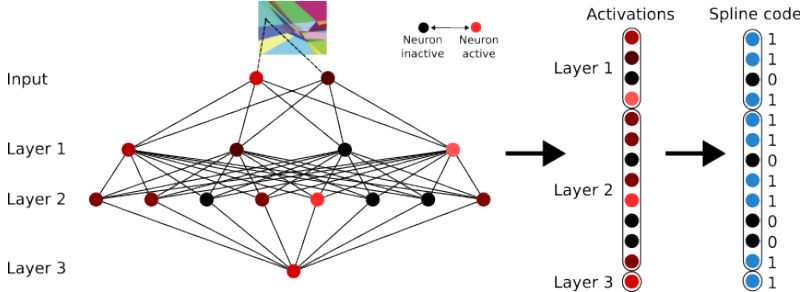


Figure 9: How spline codes are constructed in an MLP with ReLU activation functions. Activations in a set of layers are binarised according to whether each neuron is above or below threshold. (Partly adapted from Hanin and Rolnick (2019a))

At least for deep ReLU networks, polytopes provide a mathematically correct description of how the input space is partitioned, unlike the naive version of the features-as-directions view which ignores the nonlinearities. However, polytopes are far more difficult to reason about than directions. They will need to give us greater predictive power to be worth the cost.

2.1 Polytopes as the atoms of neural networks & polytope regions as their molecules

In the previous section, we discussed how it's possible (in theory) to replace an entire ReLU network with each polytope's affine transformation. Hence, polytopes provide a complete description of the input-output map of the network. Any inputs that belong to the same polytope are subject to the same affine transformation. In other words, the transformation implemented by the network is *invariant within a polytope*.

But the invariance goes even further than individual polytopes; nearby polytopes implement similar transformations. To see why, consider two polytopes that share a boundary. Their spline codes differ by *only one* neuron somewhere in the network turning on or off - in other words, the pathway taken by the activations through the network is identical except for the activation status of one neuron. Therefore, assuming the weights of some neurons aren't unusually large, polytopes that have similar spline codes implement similar transformations in expectation.⁸ Hamming distance in the space of spline codes thus corresponds to expected distance in transformation space.

It's easy to see how this might be useful for semantics: If a network needs two similar-meaning inputs to be transformed similarly, all it needs to do is to project the inputs to nearby polytopes in hidden activation space. Here, the fundamental unit of semantics in the network, which we might call a feature, is a group of nearby polytopes that implement similar transformations. Notice that the addition of polytopes only modifies the features-as-directions view without replacing it entirely: Vectors in nearby polytopes usually share high cosine similarity, so 'similar directions' will correlate with 'nearby polytopes'. Moreover, within a polytope the two views are identical.

This lets us make a few testable predictions about the relationship between semantics and polytope boundaries:

⁸This could be quantified, for instance, as the Frobenius norm of the difference matrix between the implied weight matrices of the affine transformations implemented in each polytope.

- Prediction 1: *Polysemantic directions overlap with multiple monosemantic polytope regions.*
 - The polytope lens makes a prediction about how polysemanticity is implemented in neural networks: The multiple meanings of the polysemantic direction will correspond to monosemantic regions that have nonzero inner product with that direction.
- Prediction 2: *Polytope boundaries reflect semantic boundaries*
 - Networks will learn to place more polytope boundaries between inputs of different classes than between the same classes. More generally, networks will learn to have regions denser with polytope boundaries between distinct features than between similar features.
- Prediction 3: *Polytopes define when feature-directions are on- and off-distribution.*
 - Scaling hidden activation vectors eventually causes the prediction made by a classifier to change. It should be unsurprising that scaling the activations vectors of a nonlinear network well outside their typical distribution causes the semantics of directions to break. But neither the features-as-directions perspective nor the superposition hypothesis suggest what this distribution actually is. The polytope lens predicts that polytope boundaries define this distribution. Specifically, the class prediction made by the network should tend to change when the activation vector crosses a region of dense polytope boundaries.

We find that evidence supports predictions 1 and 2, and prediction 3 appears to be only partially supported by evidence.

2.1.1 Prediction 1: Polysemantic directions overlap with multiple monosemantic polytope regions

Our approach to understanding polysemantic directions is to instead begin by identifying something in a network that *is* monosemantic and work our way out from there, rather than starting with polysemantic directions and trying to figure out how they work. So, what *is* monosemantic in a neural network?

Neural networks implement approximately smooth functions, which means that small enough regions of activation space implement similar transformations. If similar representations are transformed in similar ways, it is likely that they “mean” similar things. This implies that small enough regions of activation space should be monosemantic, and indeed - this is why techniques like nearest-neighbor search work at all. To verify this claim, here we collect together activations in a) the channel dimension in InceptionV1 and b) various MLP layers in GPT2 and cluster them using HDBSCAN, a hierarchical clustering technique.⁹ We observe that the majority of clusters found are monosemantic in both networks. For example, we observe clusters corresponding to specific types of animal in inception4c, and clusters responding to DNA strings, and specific emotional states in the later layers of GPT2-small. See Appendix E for more examples.

Instead of finding monosemantic regions by clustering activations, it’s also possible to find them by clustering spline codes. This is mildly surprising, since we’ve ostensibly removed all information about absolute magnitude - and yet it’s still possible to group similar-meaning examples together. However, a single spline code implicitly defines a set of linear constraints. These constraints, in turn, describe a set of bounding hyperplanes which confine the set of possible activations to a small region in space. Thus, much of the information about the magnitude is still retained after binarization.

We were interested in seeing if we would observe a similar effect with direction vectors found using dimensionality reduction techniques such as PCA or NMF. In theory, such directions should be those which explain the highest proportions of variance in the hidden space, and

⁹While we use HDBSCAN in this work, the specific algorithm isn’t important. Any clustering algorithm that groups together any sufficiently nearby activations or codes should yield monosemantic clusters.

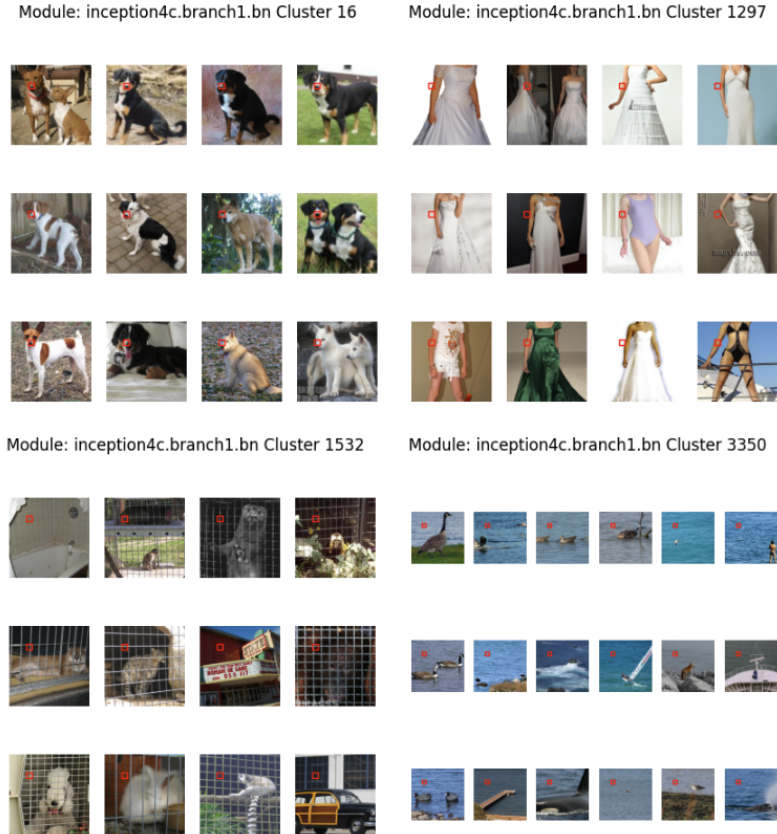


Figure 10: Examples of clusters of activations in the output of the first branch of the 4c layer of inceptionV1. For each cluster, we plot the images and hyperpixel corresponding to the activations. Clusters were computed with HDBSCAN on the activations for one spatial dimension, and randomly chosen among clusters containing enough images.

we would thus expect them to be amongst the most semantically consistent (monosemantic) ones.

In a “strong” version of the polytope lens - we might expect to see that even these directions, that we should expect to be monosemantic, also cross many polytope boundaries, potentially causing them to have different semantics at different magnitudes. However, the polytope lens does not preclude linear features - meaningful single directions are still possible in the latent space of a network with nonlinearities. To frame this in terms of paths through the network - it may be that there are linear features that are shared by all or most sets of paths.

To test this, we took the activations for a set of examples from a hidden layer (in this case, layer 4) of GPT2-small, and binarized them to get their spline codes. We then clustered the codes using HDBSCAN, with the same parameters as earlier experiments. Separately, we ran NMF on the raw activations (with 64 components) to find a set of directions. For each NMF vector, we measure the cosine similarity between it and each activation sample that we clustered, and plot the histograms in the below plots. The colours represent the cluster label that each activation has been assigned, each of which we have labelled with a semantic label by looking at the set of corresponding input samples. Since there are many clusters with extremely small cosine similarities that we are not interested in, we manually restrict the x -axis for each plot and display only the points with the largest similarities.

It turns out that the directions found using NMF do appear to be largely monosemantic - so both models observed do seem to use features associated with directions to some extent,

<p>Model: GPT2-small Layer: 0 Cluster ID: 6</p> <p>can see working but without some very complex Mecanum style wheels I can't see the VR Shoe being functional any time soon unless they have a killer new concept they've not told us about yet. I can't see one feeling balanced in this sort of get-up. ——— @pylet Pylet et (video) (https://www.youtube.com/watch?v=2N9Ht9r94) (https://www.youtube.com/watch?v=2N9Ht9r94) ——— channiboy This is still the best VR solution to running and walking, and it's already shipped. (http://www.vrml.com/http://www.vrml.com/) I just don't understand why they seem to no longer sell to consumers though. I'm not sure I</p> <p>be part of this worldwide outreach? Permission by Multi-Language Media. http://www.mml-language.com. Contact Bill Haag williamahaag@gmail.com. http://bhaag.blogspot.com. http://on.wikimedia.org/wiki/Tagalog_language... The Iron Film. Tagalog Language published:12 Oct 2008 news:26096 Clippet of John. Tagalog: https://www.youtube.com/watch?v=81Dg53pw The Biblically and historically accurate portrayal of the Life of Christ taken directly from the Gospel of Luke continues to influence the world. It has been shown in 228 countries and translated into 1031 languages as of January 2008. Also available in PAL format. Why not sponsor a language today on YouTube and be part of this worldwide outreach? Permission by Multi-Language Media. http://</p> <p>to access event. Thanks A. Put one more argument to receive in the index and will contain the event details Jddde: https://jddde.net/31anktm9/ itemClicked: function(data,index,event) { console.log('d 10' +event.currentTarget); } From KO documentation https://stackoverflow.com/documentation/click-binding.html In some scenarios, you may need to access the DOM event object associated with your click event. Knockout will pass the event as the second parameter to your function In your scenario you are binding data.index and so the last param will be event <code>function(data,index,event) { console.log('d 10' +event.currentTarget); } I am very pleased to mention publication of a relatively new book by my friends Dr. Michael Falestein (</p> <p>-12/192285/Report #: 9111 Photohttp://www.sewhaven.edu/news-events/UNH-in-the-media/2011-12/192285/2011-09-11/000000http://www.sewhaven.edu/news-events/UNH-in-the-media/2011-12/189700/9111 The Tragedy that Engulfed our Fathers http://www.sewhaven.edu/news-events/UNH-in-the-media/2011-12/189670/Academics, Researchers Help With the War on Terrorismhttp://www.sewhaven.edu/news-events/UNH-in-the</p>
<p>Model: GPT2-small Layer: 8 Cluster ID: 439</p> <p>QD signal. To validate "in vivo" detection of QD within lymph nodes, immunofluorescence staining for collagen-IV and nuclear counterstaining was performed on neck sections with QD signal using the staining protocol from Tam "et al." 2013 (10.1016/j.jid.2013.03.013). Neck sections were analyzed by confocal laser-scanning microscope (TCS SL, Leica, Germany). Identification of lymph nodes was undertaken using the nomenclature of https://doi.org/10.1016/j.jid.2013.03.013 by Van den Broeck and coworkers (1) (10.1016/j.jid.2013.03.013), with the exception that we have used the commonly accepted term of "submandibular lymph nodes" instead of "mandibular lymph nodes". Results: We "in vivo" hyperreflective imaging. QD signal was evident in the submandibular region of the right and left sides of the neck by 20 min in 5 of 7 mice and in all mice by 40</p> <p>10p006 001078_0033(ref-type="supplementary-material")** the only significant treatment effect was observed with DMA treatment. DMA impairs oxidative metabolism in infected 7774A.1 cells under IFN treatment. Cells were incubated with 300k DNA for 24 h and infected with 20 MOI of vBp1. Reactive oxygen intermediates were estimated by FACS. https://doi.org/10.1016/j.jid.2013.03.013 in the (Materials and Methods)(10.1016/j.jid.2013.03.013). ** Quantitative data about the relative percentage of EB red fluorescence (mean ± SEM): https://doi.org/10.1016/j.jid.2013.03.013. * Indicates a significant effect of DNA compared to Control. ** P<0.05. Abbreviations used: DNA, deoxythionucleic acid; EB, ethidium bromide.</p> <p>10p found that 9.3% of patients with >60% DI still showed an incomplete recovery. What's more, the ENOG cutoff value in our study is also different from others (10.1016/j.jid.2013.03.013). From this regard, for the patients with ENOG DI between 60% and 90%, it is doubtful that whether a surgical treatment is necessary. All in all, further research is required to confirm conclusions and hypotheses. https://doi.org/10.1016/j.jid.2013.03.013 above, since there are biases in patient selection, the examination time from the onset of symptoms, definition of functional recovery, and follow-up time. There was significant correlation between the value of PLT and poor outcome of RP but not RRS. Also in our study, there was no significant difference in initial PLT values between RP and RRS. We speculated that it may result from different underlying pathogenesis of 2 disorders. RRS is caused by latent varicella-z</p> <p>TOTAL 3751 These regions/states with no matches with Roma sequences (probability https://doi.org/10.1016/j.jid.2013.03.013 with hypoten c). The subcontinental region showing higher probability of being the source of Roma sequences was North-western India (0.72), followed by Eastern India (0.20) while the rest of the subcontinental regions accounted only for 0% of the probability. When the analysis was performed at state level, results pointed at Punjab state (in North-Western India) as the most probable candidate to be the ancestral homeland of the Roma mtDNA types (probability https://doi.org/10.1016/j.jid.2013.03.013)</p> <p>by deletion of E1 sequences and substitution of foreign DNA, and are produced in complementing human cell lines that constitutively express E1 proteins. Graham et al. (1977). J. Gen. Virol. 36:59-74; Fallas et al. (1996). Hum. Gene Ther. 7:215-222; Fallas et al. (1998). Hum. Gene Ther. 9:1909-1917. An adenovirus E1A region https://doi.org/10.1016/j.jid.2013.03.013 in Duryabzhe (1996). Nature 211:102 and Whyte et al., 1988. J. Virol. 62:257-269. Though E1-deleted viruses do not replicate in cells that do not express E1 proteins, the viruses can express foreign proteins in these cells, provided the genes are placed under the control of a constitutive promoter. Xiang et al. (1996). Virology 219:220-227. Vaccination of animals with adenov</p>
<p>Model: GPT2-small Layer: 8 Cluster ID: 417</p> <p>medium in the presence of 5 µg/ml of cyclohalasin B. After activation, embryos were cultured in KSOMaa medium for 4.5-5.5 days. Zygotes from naturally bred mice were used as control. Differences in blastocyst formation rate and blastocyst cell number among treatments were analyzed by one-way ANOVA after acinar square transformation. In the first experiment, blastocyst formation rate in the first group was higher than in the second (69.6±6.9 vs. 47.1±9.0; P<0.05). In addition, blastocyst cell number was also higher in the first group than in the second one (69.4±3.2 vs. 52.4±2.2; P<0.05). However, both values were higher in control group (80.9; 76.2±1.2; P<0.05) than in the experimental groups. These results showed that young o</p> <p>were compared with those of 659 PMBV performed with the double-balloon technique. Baseline clinical and morphologic characteristics between early and late experience Inoue groups were similar. Post-PMBV mitral valve area (1.89±0.056 vs. 1.69±0.057 cm²; p=0.008) and success rate (69% vs. 75.9%; p=0.009) were significantly higher in the late experience Inoue group. Furthermore, there was a trend for less incidence of severe post-PMBV mitral regurgitation (>=3+ in the late experience group (0.8% vs. 12%; p=0.16). Although the post-PMBV mitral valve area was larger with the double-balloon technique (1.94±0.072 vs. 1.81±0.08 cm²; p=0.01), the success rate (71.3</p> <p>were evaluated before and during the 24 h after study drug administration. Complete response to placebo, changes (no vomiting and/or reching, and no rescue antimetics over the initial 0-24 period) was more frequent in the endosome groups (1 mg 57%, 4 mg 61%, and 8 mg 57%) than in the placebo group (30%, P<0.001). For the 0-24 h study a complete response occurred in only 15% of the placebo group compared to 41%, 47%, and 47% of the 1-, 4-, and 8-mg endosome groups, respectively (P<0.001 for all comparisons with placebo). Median nausea scores (range 0-10) during the initial observation period (0-2 h) were significantly lower for all doses of ondansetron (1.3, 0.8, 1.8 for 1-, 4-, and 8 mg, respectively) as compared with placebo (2</p> <p>12-182090) as a cutoff (data available upon request from the corresponding author). Compared to placebo, changes from baseline in total RIL-AG score, RIL-A response, PNA, and SLEDA4 were greater for patients with a CRP concentration higher than the median value. **Immunologic response.** By week 48 in the EMBODY trials, a reduction in B cell count from baseline of between 30% and 40% was observed in SLE patients receiving granatamab. Consistent with these results, a reduction in CD19+ B cell count of between 30% and 40% was observed in both patients without associated SS and patients with associated SS receiving granatamab, but not those receiving placebo (figure 12)(10.40425-5g-0002)(ref-type="fig")A and B). No differences were seen between patients with associated SS and those without associated SS. †</p> <p>to treatment failure or lack of adherence to the treatment. The weak association between age acceleration and viral load may reflect the fact that viral load does not capture the history of viral load burden. Controlled in vitro studies would be helpful for understanding the relationship between viral load and age acceleration. In conclusion, we demonstrate that HIV infection is associated with a significant increase in DNA methylation age in brain and blood tissue. Our results are consistent with the reported clinical manifestations of accelerated aging effects among HIV-infected https://doi.org/10.1016/j.jid.2013.03.013 despite apparent viral control. Future studies will need to explore whether the epigenetic clock can serve as a useful tool for the study of and/or inform therapeutic strategies aimed at preventing HIV-associated non-AIDS-defining conditions such as cardiovascular disease and HIV-associated neurocognitive disorder (10.1016/j.jid.2013.03.013). Supplementary Data (MS) https://doi.org/10.1016/j.jid.2013.03.013 [Supplementary materials](http://)</p>

Figure 12: Dataset examples of clusters in the pre-activations of the MLP in various layers of GPT2-small. Clusters were computed using HDBSCAN on a random sample of the pile's test set. The distance matrix for clustering in the above examples was computed using hamming distance on the binarized spline codes. Each token in the test set is treated as a separate point for clustering, and the specific token that has been clustered has been highlighted in red in each instance. We observe specific clusters in earlier layers that appear to be related to detokenization - i.e grouping "http" and "https" together. Clusters later layers tend to respond to higher level semantics - synonyms for groups of patients in medical trials, for example.

even if the basis directions still appear highly polysemantic. Using the same procedure, we can also find these monosemantic directions in InceptionV1:

The above experiments suggest that there do exist feature directions which are coherent across all polytopes in some specific layer - meaning that the affine transformations formed across the set of all polytopes are sufficiently similar to some extent.

2.1.2 Prediction 2: Polytope boundaries reflect semantic boundaries

Why should we expect polytope boundaries to reflect semantic boundaries? One geometric intuition underlying this idea is that nonlinearities are needed to silence interference between

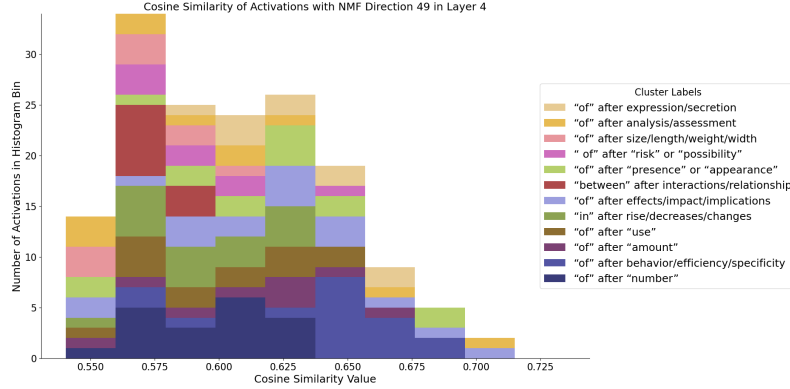


Figure 13: Cosine similarities with respect to NMF direction 49. Activations taken from the MLP in layer 4 of GPT2-Small, using data from The Pile’s test set . The dataset examples with the highest cosine similarities are shown and coloured by their cluster label (ignoring the smallest clusters).

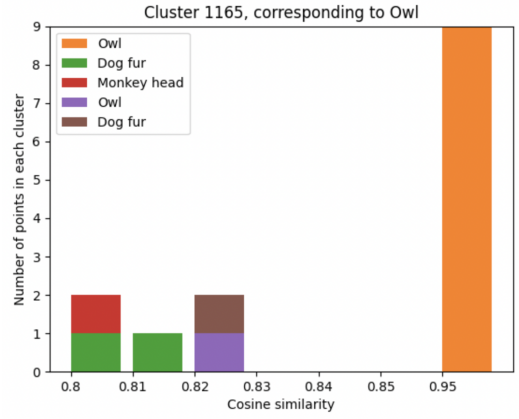


Figure 14

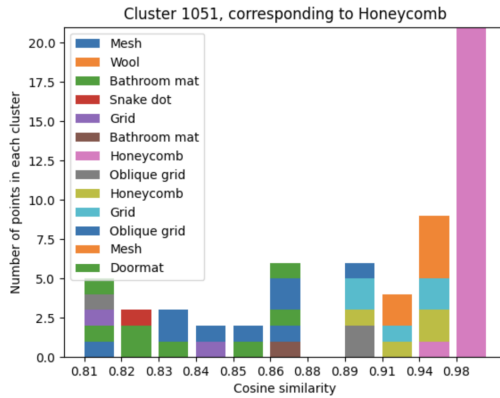


Figure 15

non-orthogonal features in superposition. Polytope boundaries should therefore be placed between non-orthogonal feature directions so that activations in one feature direction don’t activate the other when they shouldn’t. Another intuition is that neural networks are often used in situations where outputs are not linearly separable functions of the inputs, such as image classification. To solve such tasks, neural networks fold and squeeze the input data manifold into a shape that is linearly separable in subsequent layers (Keup and Helias, 2022).

Affine transformations on their own cannot improve linear separability - but since a ReLU activation maps negative values to zero, it can be thought of as making a fold in the data distribution, with the position of the dent being controlled by the previous transformation's weights. Several ReLU neurons in combination can also act to expose inner class boundaries - making classification in later layers possible where it wasn't in earlier ones - by "folding" regions of the distribution into new, unoccupied dimensions (see the figure below for a 1D geometric interpretation). For this reason we may expect to see a concentration of ReLU hyperplanes around such distributions, as the network acts to encode features for later layers.

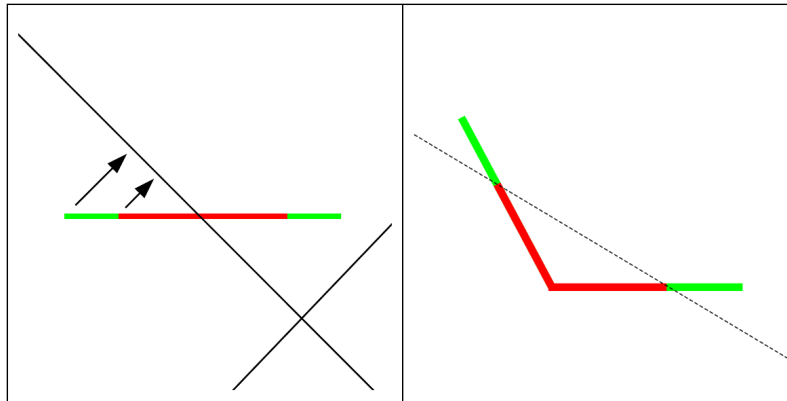


Figure 16: How a ReLU neuron can act to expose a previously non-separable class boundary, reproduced from Keup and Helias, (2022). The solid black line is a ReLU hyperplane, and the dashed line represents a potential decision boundary. In higher dimensions - this effect requires several ReLU hyperplanes to act in conjunction.

Images of different classes will have many different features. Therefore, according to the polytope lens, activations caused by images from different classes should be separated by regions of denser polytope boundaries than those caused by images from the same class. Can we see this by looking at heat map visualizations of polytope density? Unfortunately, the network has too many neurons (and thus too many boundaries) to observe any differences directly.

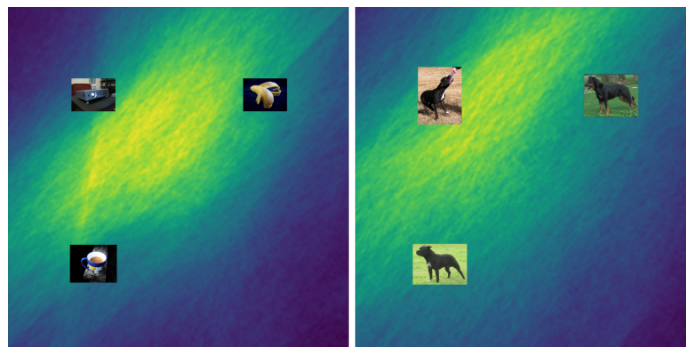


Figure 17: Heat maps of polytope density in a 2-D slice through the 40,768-dimensional input space of layer inception5a. The 2-D slice was made such that the activation vectors of three images lie on the plane. Then we calculated the spline codes (using layers inception5a to the output) for every point in a $4,096 \times 4,096$ grid. Then we computed the Hamming distance between codes in adjacent pixels and applied a Gaussian smoothing. Observe that the densest region is the part of the image separating the three inputs. Method adapted from Novak et al. (2018), who calculated similar images for small networks.

But when we measure the polytope densities directly (by dividing the distance between two activation vector's spline codes by their Euclidean distance, it indeed turns out to be the

case that activations caused by images of different classes are separated by regions denser in polytope boundaries than activations caused by images of the same class:

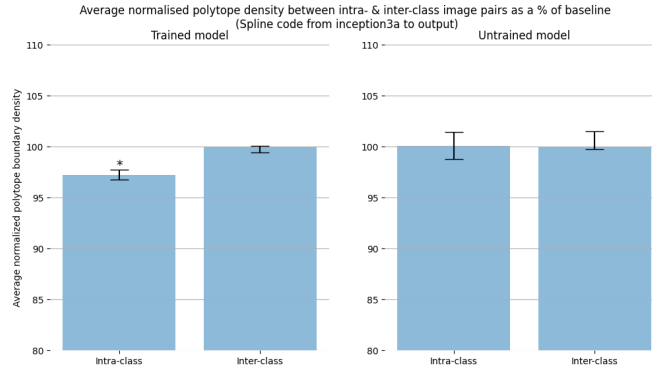


Figure 18: The average normalized polytope boundary density between the activation vector caused by images of the same or different classes. The left plot is for a trained network; the right an untrained network. Since images of different classes will also produce distant activations, we should consider the density of polytope boundaries rather than the absolute number of polytope boundaries between the activations produced by different images. To calculate the polytope boundary density between two points, we simply divide the Hamming distance in between their spline codes by the Euclidean distance between them. The polytope densities are normalized by dividing by the average polytope density between all pairs of vectors (both intra and inter class). Only for the trained network is the intra-class polytope density lower. This difference increases as we move higher in the network (Figure below). The error bars are 99% bootstrapped confidence intervals. A single asterisk indicates a statistically significant difference according to a Welch’s t -test ($t(1873.3) = -14.7$; $p = 3.8e - 46$). Note the y -axis begins at 80%; the difference is small, but significant. We see a similar story when we interpolate (instead of simply measuring the total distances) between two images of the same or different classes (Appendix A).

The intra- and inter-class difference is small, but significant. The difference gets more robust as we look at higher layers. The polytope lens predicts this because activations in lower layers represent low level features, which are less informative about image class than features in higher layers. For example, two images of dogs might be composed of very different sets of lines and curves, but both images will contain fur, a dog face, and a tail. Because there are more irrelevant features represented in lower layers, the percentage of polytope boundaries that relate features that are relevant to that class is smaller than between features represented in higher layers.

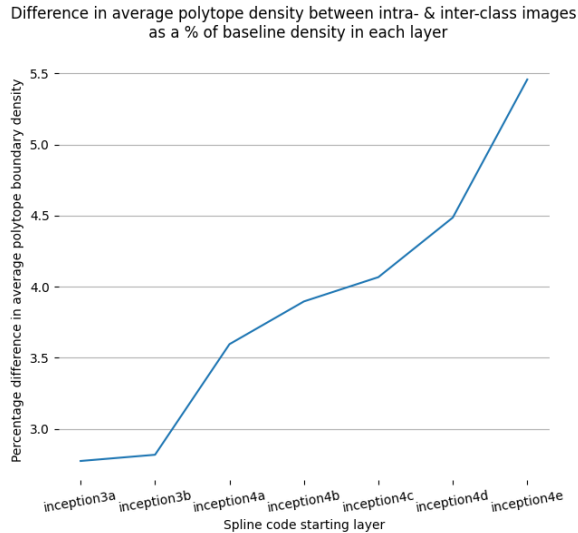


Figure 19: The difference between the normalized polytope density between intra- and inter-class images gets larger in layers closer to the output.

2.1.3 Prediction 3: Polytopes define when feature-directions are on- and off-distribution

One of the responses to the scaling activations experiments that we’ve encountered is that we’re being unfair to the networks: We shouldn’t expect their semantics to remain intact so far outside of their typical distribution. We agree! That there exists such a distribution of validity is, in fact, a central motivation for looking at networks through the polytope lens.

The features-as-directions hypothesis doesn’t by itself make claims about the existence of a distribution of semantic validity because it assumes that representations are linear and therefore globally valid. The polytope lens predicts that scaling an activation vector will change the semantics of a given direction only when it crosses many polytope boundaries. It makes this prediction because the larger the distance between two polytopes, the more different (in expectation) is the transformation implemented by them. Polytopes boundaries thus suggest a way to identify the distribution of semantic validity.

Is this the case empirically? Partially. When we plot the local polytope density in the region near the scaled vector, we see that there is a characteristic peak between the activation vector and the origin. This peak occurs even for activation directions defined by Gaussian noise, but is absent in untrained networks (Appendix B). There appears to be a ‘shell’ of densely packed polytope boundaries surrounding the origin in every direction we looked. We’re not completely sure why polytope boundaries tend to lie in a shell, though we suspect that it’s likely related to the fact that, in high dimensional spaces, most of the hypervolume of a hypersphere is close to the surface. Scaling up the activation, we see that the vector crosses a decreasing number of polytope boundaries. This is what you’d expect of polytope boundaries that lie near the origin and extend to infinity; as a result, polytopes further from the origin will be made from boundaries that become increasingly close to being parallel. Therefore a vector crosses fewer polytope boundaries as it scales away from the center. We nevertheless see plenty of class changes in regions that are distant from the origin that have low polytope density. This wasn’t exactly what the polytope lens predicted, which was that dense polytope boundaries would be located where there were class changes. Instead we observed dense polytope boundaries as we scale *down* the activity vector and not as we scale it up. It appears that polytope boundaries only demarcate the inner bound of the distribution where a given direction means the same thing. That class changes can be observed for large magnitude activation vectors despite a low polytope boundary might simply reflect that it’s easier for large magnitude activations to move large distances when the transformations they undergo are small.

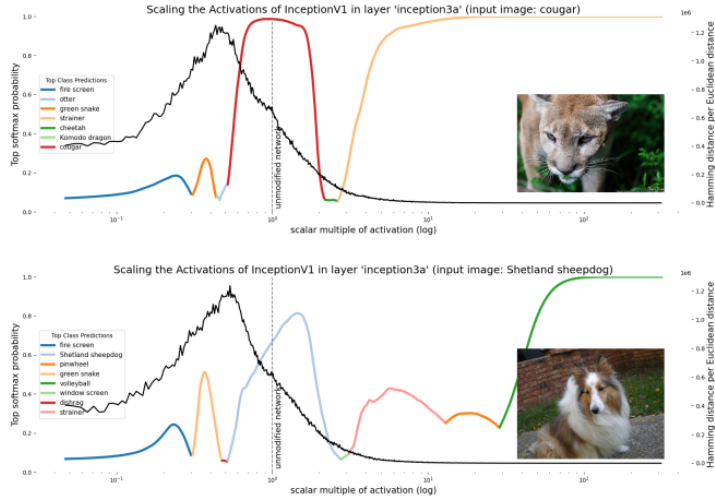


Figure 20: The polytope density (black line) overlaying the class logits (coloured lines) for two images where the activation in a hidden layer - inception3a - is scaled. Polytope density peaks around halfway between the unscaled activation vector and the origin.

So polytope boundaries reflect - to some extent - the semantics learned by the network; they capture transformational invariances in the network, reflect feature boundaries, and seem to demarcate the inner bound of where feature-directions should be considered on- or off-distribution. They also seem to be involved in “encoding” features from raw data. Polytopes thus have many excellent properties for describing what is going on inside neural networks - but, as we will discuss in the next section, it’s not clear how to harness polytopes to create [Decomposable](#) descriptions of the features in a network. Whilst studying neural networks through their polytope regions is a more “complete” description in some sense, it does not (so far) let us understand network representations in terms of features that can be understood independently.

3 Discussion

Our effort to account for nonlinearities in neural networks has forced us to consider not just the direction of neural activations, but also their scale. This is because nonlinearities behave differently at different activation scales. Polytopes offer a way to think about how networks use nonlinearities to implement different transformations at different activation scales. But with many neurons comes exponentially many polytopes. Spline codes present a scalable way to talk about the exponential number of polytopes in neural networks since we can talk about “groups” or “clusters” of spline codes instead of individual codes.

Unfortunately, accounting for nonlinearities in this way has cost us rather a lot. Instead of dealing with globally valid feature directions, we now deal with only locally valid feature directions in activation space. By studying the structure of spline codes rather than the structure of activations, polytopes offer us the ability to identify regions of activation space that have roughly similar semantics. Are the costs worth the gains?

The short answer is that we’re not sure. The polytope lens is a way to view neural networks that puts nonlinearities front and center; but if neural networks use primarily linear representations (as hypothesized by [Elhage et al. \(2022\)](#)), then such a nonlinearity-focused perspective could potentially offer relatively little compared to a purely linear perspective, since the abstraction of a globally valid feature direction will not be particularly leaky. The lesson we take from observations of superposition and polysemanticity is that networks are often not operating in the linear regime; they suggest that they are making nontrivial use of their nonlinearities to suppress interference from polysemantic directions. This is also suggested by the empirical performance of large networks which substantially exceeds the equivalent purely linear models. It therefore appears that we need a way to account for

how different regions of activation space interact differently with nonlinearities and how this affects the semantics of the network’s representations.

We ultimately think that mechanistic descriptions of networks with superposition which take nonlinearity into account will look somewhat different from previous mechanistic descriptions that tended to assume linearity (Elhage et al., 2022). The polytope lens might represent an important component of such descriptions, but we’re in no way certain. If it were, what might mechanistic descriptions of neural networks look like through the polytope lens?

We think a potentially important idea for describing what neural networks have learned might be ‘**representational flow**’ between polytope regions. The input space of a layer may have regions that are semantically similar yet spatially distant and the job of the network is to learn how to project these spatially distant points to similar regions of output space. For example, the two images of cats in Figure 21(a) below are distant in input space yet semantically similar in output space; the network performs **representational convergence** between representations in the input and output spaces. Representational convergence may also happen between arbitrary layers, such as between the input space and layer L if the inputs happen to share features that are represented in that layers’ semantic space (Figure 21(b)). The converse is also possible: A network implements **representational divergence** if spatially similar inputs are semantically different from the perspective of the network at layer L (Figure 21(c)). In order to implement representational *convergence*, different polytopes need to have affine transformations that project them to similar parts of the space in later layers. Conversely, representational *divergence* requires transformations that project nearby regions of activation space to distant regions in the spaces of later layers. Networks achieve both of these things by having the right affine transformations associated with the polytope regions involved. Nonlinearities mean that vectors that have an identical direction but different scales can take different pathways through the network. The benefit of thinking about networks in terms of representational flow is that it therefore allows us to talk about the effects of nonlinearities on activation directions of different scales.

Recent work on superposition by Elhage et al. (2022) argues that models with superposition will only be understood if we can find a sparse overcomplete basis (or if we remove superposition altogether, an option we don’t consider here). Finding this basis seems like a crucial step toward understanding, but we don’t think it’s the full story. Even if we could describe a layer’s input features in terms of a sparse overcomplete basis, each combination of those sparse feature directions will have different patterns of interference which each interact differently with the nonlinearities. Thus, the elements of the sparse basis that are active will vary depending on the input vector; we therefore haven’t found a way around the issue that nonlinearities force us to use local, rather than global, bases.

Consequently, for most combinations it’s hard to predict exactly which activations will be above threshold without calculating the interference terms and observing empirically which are above or below threshold; this is a problem for mechanistic interpretability, where we’d like to be able to mentally model a network’s behavior without actually running it. Therefore, a sparse overcomplete basis by itself wouldn’t let us avoid accounting for nonlinearities in neural networks. Introducing assumptions about the input distribution such that interference terms are always negligibly small might however let us make predictions about a network’s behavior without adding schemes, like polytopes, that attempt to account for nonlinearities.

Our work is more closely related to the search for an overcomplete basis than it might initially appear. Clustering activations can be thought of as finding a k -sparse set of features in the activations where $k = 1$ (when k is the number of active elements). In other words, finding N clusters is equivalent to finding an overcomplete basis with N basis directions, only one of which can be active at any one time. This clearly isn’t optimal for finding decomposable descriptions of neural networks; ideally we’d let more features be active at a time i.e. we’d like to let $k > 1$, but with clustering $k = 1$. But clustering isn’t completely senseless - If every combination of sparse overcomplete basis vectors interacts with nonlinearities in a different way, then every combination *behaves* like a different feature. Fortunately, even if it were true that every combination of sparse overcomplete features interacted with nonlinearities in

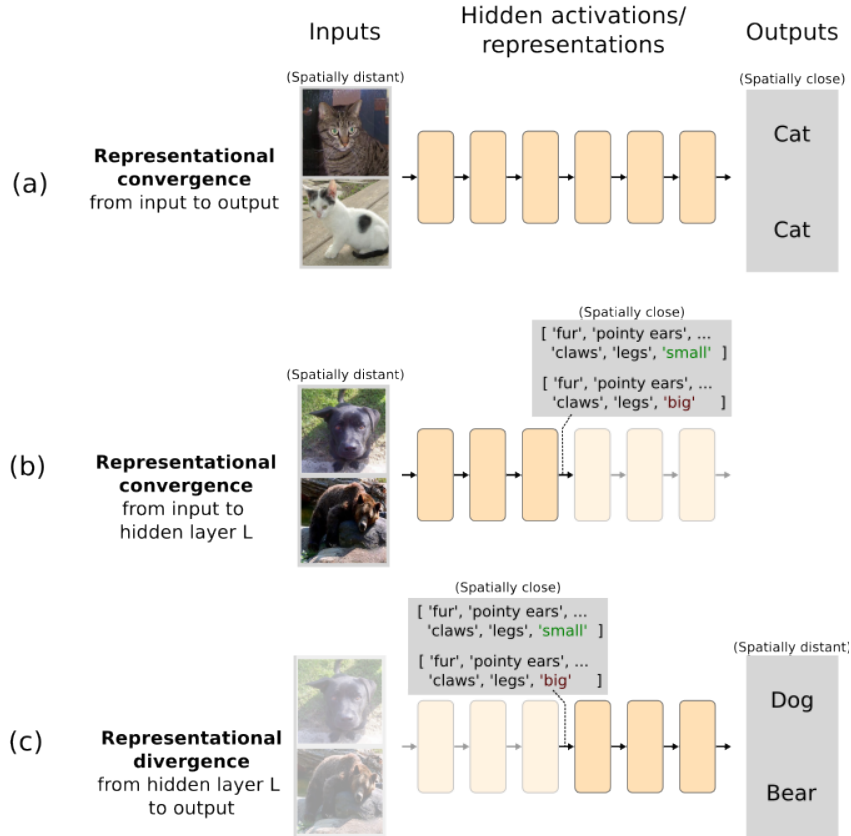


Figure 21: Representational flow between polytope regions might be a useful notion in mechanistic descriptions of neural networks.

a different way, their interactions almost definitely have statistical and geometric structure, which we might be able to understand. Overcomplete basis features will be one component of that structure, but they don't account for scale; polytopes do. A path toward understanding superposition in neural networks might be an approach that describes it in terms of an overcomplete basis *and* in terms of polytopes. A potential future research direction might therefore be to find overcomplete bases in spline codes rather than simply clustering them. This might be one way to decompose the structure of representational flow into modules that account for both activation directions as well as activation scale.

Many other questions remain unaddressed in this post. We think they will be important to answer before the polytope lens can be used in as many circumstances as the features-as-directions perspective has been.

- **Fuzzy polytope boundaries with other activations** - For the sake of simplicity, we've been assuming that the networks discussed in the article so far have used piecewise linear activation functions such as ReLU. But many networks today, including large language models, often use smooth activations such as GELU and softmax, which mean that their polytopes won't really be polytopes - their edges will be curvy or even 'blurred'. Some prior work exists that extends the polytope lens to such activations (Balestrierio and Baraniuk, 2018b). See Appendix C for further discussion.
- **How do we extend the polytope lens to transformers?** Specifically, how should we talk about polytopes when attention between embedding vectors makes activations (and hence polytopes) interact multiplicatively across sequence positions?

- **How do adversarial examples fit into this picture?** Are adversarial examples adversarial because they perturb the input such that it crosses many polytope boundaries (polytope ridges)? And can we use this potential insight in order to make networks less susceptible to such attacks?

4 Related work

4.1 Interpreting polytopes, single neurons, or directions

The geometric interpretation of ReLU networks was, to our knowledge, first laid out by [Nair and Hinton \(2010\)](#), who note that each unit corresponds to a hyperplane through the input space, and that N units in concert can create 2^N regions (what we call polytopes), each of which can be viewed as a separate linear model. [Pascanu et al. \(2014\)](#) undertook a more detailed theoretical analysis of the number of these linear regions in ReLU models.

The fact that each of these regions could be identified as a unique *code*, which can then be used for interpretability analysis and clustering, was explored by [Srivastava et al. \(2015\)](#), who studied a small MNIST network by clustering the codes at its final layer.

That these regions take the form of convex polytopes is also not a novel concept, and has been explored in a number of prior works ([Balestriero and Baraniuk, 2018a](#); [Novak et al., 2018](#); [Hanin and Rolnick, 2019b](#); [Rolnick and Kording, 2020](#); [Xu et al., 2022](#)). In this writeup, we have relied particularly heavily on conceptualizing DNNs as compositions of *max-affine spline operators*, as introduced in [Balestriero and Baraniuk \(2018a\)](#), and expanded upon in a series of further works ([Balestriero and Baraniuk, 2018b](#); [Balestriero et al., 2019](#)).

However, in much of the wider interpretability field – particularly in papers focused on interpretability in language models – this point of view has gone largely unnoticed, and interpretation efforts have tended to try to identify the role of single neurons or linear combinations of neurons (directions). Interpretable neurons have been noted fairly widely in various works focusing on vision models ([Szegedy et al., 2014](#); [Bau et al., 2017](#)). Interpretable directions were also a central focus of the [Circuits Thread](#), ([Camarata et al., 2020b](#)), where they used knowledge built up from interpreting neurons in early layers of inceptionv1 to hand code curve detectors that, when substituted for the curve detectors in the original network, induced minimal performance loss.

Interpretable single neurons have also been found in language models ([Geva et al., 2021](#); [Durrani et al., 2020](#); [Dai et al., 2022](#); [Elhage et al., 2022](#)), although monosemantic neurons seem comparatively less common in this class of model. [An Interpretability Illusion for BERT \(Bolukbasi et al., 2021\)](#), highlighted the fact that the patterns one might see when inspecting the top- k activations of some neuron may cause us to spuriously interpret it as encoding a single, simple concept, when in fact it is encoding for something far more complex. They also noted that many directions in activation space that were thought to be globally interpretable may only be locally valid.

4.2 Polysemanticity and Superposition

The earliest mention of polysemanticity we could find in machine learning literature was from [Nguyen et al. \(2016\)](#). In their paper they identify the concept of *multifaceted* neurons. That is, neurons which fire in response to many different types of features. In this work, we define *polysemantic* neurons as neurons which fire in response to many different *unrelated* features, and they identify an example of this in their supplementary material (Figure S5).

Work by [Olah et al. \(2017\)](#), [Feature Visualization](#), identified another way to elicit polysemantic interpretations and helped to popularize the idea. They note that, as well as there being neurons which represent a single coherent concept, “...there are also neurons that represent strange mixtures of ideas. Below, a neuron responds to two types of animal faces, and also to car bodies. Examples like these suggest that neurons are not necessarily the right semantic units for understanding neural nets.”

Even before this, the possibility that individual neurons could respond to multiple features was discussed in some early connectionist literature, including [Hinton \(1981\)](#). In neuro-



Figure 22: Image from Olah et al. (2017) depicting a polysemantic neuron.

science, polysemanticity is usually called ‘mixed selectivity’. Neuroscience has only in the last decade or two developed the tools required to identify and study mixed selectivity. Since then, it has been the subject of increasing attention, especially its role in motor- and decision- neuroscience (Churchland and Shenoy, 2007; Rigotti et al., 2013; Mante et al., 2013). For a review of mixed selectivity in neuroscience, see Fusi et al. (2016).

Recent work from Elhage et al. (2022) sheds light on a phenomenon that they term “superposition”. Superposition occurs when a neural network represents more features than it has dimensions, and the mapping from features to orthogonal basis directions can no longer be bijective. This phenomenon is related to, but not the same as polysemanticity; it may be a cause of some of the polysemantic neurons we see in practice. They investigate toy models with non-linearities placed at the output layer, and show that superposition is a real phenomenon that can cause both mono- and polysemantic neurons to form. They also describe a simple example of computation being performed on features in superposition. Finally, they reveal that superposition can cause a different type of polytope to form - in their toy model, features are organized into geometric structures that appear to be a result of a repulsive force between feature directions which acts to reduce interference between features. It’s worth emphasizing that the polytopes discussed in their work aren’t the same kind as in ours: For one, our polytopes lie in activation space whereas theirs lie in the model weights. Perhaps a more fundamental divergence between Elhage et al.’s model and ours is the assumption of linearity - the idea that features are represented by a single direction in activation space. As we explained in earlier sections, we believe that assuming linearity will yield only partial mechanistic understanding of nonlinear networks. While globally valid feature directions would simplify analysis, in practice we struggle to see a way around nonlinearity by assuming linear representations.

Acknowledgments and Disclosure of Funding

This work benefited from feedback from many staff at Conjecture including Adam Shimi, Nicholas Kees Dupuis, Dan Clothiaux, Kyle McDonell. Additionally, the post also benefited from inputs from Jessica Cooper, Eliezer Yudkowsky, Neel Nanda, Andrei Alexandru, Ethan Perez, Jan Hendrik Kirchner, Chris Olah, Nelson Elhage, David Lindner, Evan R Murphy, Tom McGrath, Martin Wattenberg, Johannes Treutlein, Spencer Becker-Kahn, Leo Gao, John Wentworth, and Paul Christiano and from discussions with many other colleagues working on interpretability.

References

- Y. Abu-Mostafa and J. St. Jacques. Information capacity of the Hopfield model. *IEEE Transactions on Information Theory*, 31(4):461–464, July 1985. ISSN 0018-9448. doi: 10.1109/TIT.1985.1057069. URL <http://ieeexplore.ieee.org/document/1057069/>.
- Randall Balestriero and richard baraniuk. A spline theory of deep learning. In Jennifer Dy and Andreas Krause, editors, *Proceedings of the 35th international conference on machine learning*, volume 80 of *Proceedings of machine learning research*, pages 374–383. PMLR, July 2018. URL <https://proceedings.mlr.press/v80/balestriero18b.html>. tex.pdf: <http://proceedings.mlr.press/v80/balestriero18b/balestriero18b.pdf>.
- Randall Balestriero and Richard Baraniuk. Mad Max: Affine Spline Insights into Deep Learning, November 2018a. URL <http://arxiv.org/abs/1805.06576>. arXiv:1805.06576 [cs, stat].

- Randall Balestriero and Richard G. Baraniuk. From Hard to Soft: Understanding Deep Network Nonlinearities via Vector Quantization and Statistical Inference, October 2018b. URL <http://arxiv.org/abs/1810.09274>. arXiv:1810.09274 [cs, stat].
- Randall Balestriero, Romain Cosentino, Behnaam Aazhang, and Richard Baraniuk. The Geometry of Deep Networks: Power Diagram Subdivision, May 2019. URL <http://arxiv.org/abs/1905.08443>. arXiv:1905.08443 [cs, stat].
- David Bau, Bolei Zhou, Aditya Khosla, Aude Oliva, and Antonio Torralba. Network dissection: Quantifying interpretability of deep visual representations. In *Computer vision and pattern recognition*, 2017.
- Tolga Bolukbasi, Adam Pearce, Ann Yuan, Andy Coenen, Emily Reif, Fernanda Viégas, and Martin Wattenberg. An Interpretability Illusion for BERT, April 2021. URL <http://arxiv.org/abs/2104.07143>. arXiv:2104.07143 [cs].
- Nick Cammarata, Shan Carter, Gabriel Goh, Chris Olah, Michael Petrov, and Ludwig Schubert. Thread: Circuits. *Distill*, 5(3):10.23915/distill.00024, March 2020a. ISSN 2476-0757. doi: 10.23915/distill.00024. URL <https://distill.pub/2020/circuits>.
- Nick Cammarata, Shan Carter, Gabriel Goh, Chris Olah, Michael Petrov, Ludwig Schubert, Chelsea Voss, Ben Egan, and Swee Kiat Lim. Thread: Circuits. *Distill*, 2020b. doi: 10.23915/distill.00024.
- Nick Cammarata, Gabriel Goh, Shan Carter, Ludwig Schubert, Michael Petrov, and Chris Olah. Curve detectors. *Distill*, 2020c. doi: 10.23915/distill.00024.003.
- Nick Cammarata, Gabriel Goh, Shan Carter, Chelsea Voss, Ludwig Schubert, and Chris Olah. Curve circuits. *Distill*, 2021. doi: 10.23915/distill.00024.006.
- Mark M. Churchland and Krishna V. Shenoy. Temporal Complexity and Heterogeneity of Single-Neuron Activity in Premotor and Motor Cortex. *Journal of Neurophysiology*, 97(6):4235–4257, June 2007. ISSN 0022-3077, 1522-1598. doi: 10.1152/jn.00095.2007. URL <https://www.physiology.org/doi/10.1152/jn.00095.2007>.
- Damai Dai, Li Dong, Yaru Hao, Zhifang Sui, Baobao Chang, and Furu Wei. Knowledge Neurons in Pretrained Transformers, March 2022. URL <http://arxiv.org/abs/2104.08696>. arXiv:2104.08696 [cs].
- Nadir Durrani, Hassan Sajjad, Fahim Dalvi, and Yonatan Belinkov. Analyzing Individual Neurons in Pre-trained Language Models, October 2020. URL <http://arxiv.org/abs/2010.02695>. arXiv:2010.02695 [cs].
- Nelson Elhage, Neel Nanda, Catherine Olsson, Tom Henighan, Nicholas Joseph, Ben Mann, Amanda Askell, Yuntao Bai, Anna Chen, Tom Conerly, Nova DasSarma, Dawn Drain, Deep Ganguli, Zac Hatfield-Dodds, Danny Hernandez, Andy Jones, Jackson Kernion, Liane Lovitt, Kamal Ndousse, Dario Amodei, Tom Brown, Jack Clark, Jared Kaplan, Sam McCandlish, and Chris Olah. A mathematical framework for transformer circuits. *Transformer Circuits Thread*, 2021.
- Nelson Elhage, Tristan Hume, Catherine Olsson, Nicholas Schiefer, Tom Henighan, Shauna Kravec, Zac Hatfield-Dodds, Robert Lasenby, Dawn Drain, Carol Chen, Roger Grosse, Sam McCandlish, Jared Kaplan, Dario Amodei, Martin Wattenberg, and Christopher Olah. Toy models of superposition. *Transformer Circuits Thread*, 2022.
- Stefano Fusi, Earl K Miller, and Mattia Rigotti. Why neurons mix: high dimensionality for higher cognition. *Current Opinion in Neurobiology*, 37:66–74, April 2016. ISSN 09594388. doi: 10.1016/j.conb.2016.01.010. URL <https://linkinghub.elsevier.com/retrieve/pii/S0959438816000118>.
- Mor Geva, Roei Schuster, Jonathan Berant, and Omer Levy. Transformer Feed-Forward Layers Are Key-Value Memories, September 2021. URL <http://arxiv.org/abs/2012.14913>. arXiv:2012.14913 [cs].
- Gabriel Goh, Nick Cammarata †, Chelsea Voss †, Shan Carter, Michael Petrov, Ludwig Schubert, Alec Radford, and Chris Olah. Multimodal neurons in artificial neural networks. *Distill*, 2021. doi: 10.23915/distill.00030.

- Boris Hanin and David Rolnick. Complexity of linear regions in deep networks. In Kamalika Chaudhuri and Ruslan Salakhutdinov, editors, *Proceedings of the 36th international conference on machine learning*, volume 97 of *Proceedings of machine learning research*, pages 2596–2604. PMLR, June 2019a. URL <https://proceedings.mlr.press/v97/hanin19a.html>. tex.pdf: <http://proceedings.mlr.press/v97/hanin19a/hanin19a.pdf>.
- Boris Hanin and David Rolnick. Deep ReLU Networks Have Surprisingly Few Activation Patterns, October 2019b. URL <http://arxiv.org/abs/1906.00904>. arXiv:1906.00904 [cs, math, stat].
- Geoffrey F. Hinton. Shape representation in parallel systems. In *Proceedings of the 7th international joint conference on artificial intelligence - volume 2*, IJCAI’81, pages 1088–1096, San Francisco, CA, USA, 1981. Morgan Kaufmann Publishers Inc. Number of pages: 9 Place: Vancouver, BC, Canada.
- J J Hopfield. Neural networks and physical systems with emergent collective computational abilities. *Proceedings of the National Academy of Sciences*, 79(8):2554–2558, April 1982. ISSN 0027-8424, 1091-6490. doi: 10.1073/pnas.79.8.2554. URL <https://pnas.org/doi/full/10.1073/pnas.79.8.2554>.
- D. H. Hubel and T. N. Wiesel. Receptive fields, binocular interaction and functional architecture in the cat’s visual cortex. *The Journal of Physiology*, 160(1):106–154, January 1962. ISSN 00223751. doi: 10.1113/jphysiol.1962.sp006837. URL <https://onlinelibrary.wiley.com/doi/10.1113/jphysiol.1962.sp006837>.
- Christian Keup and Moritz Helias. Origami in N dimensions: How feed-forward networks manufacture linear separability, March 2022. URL <http://arxiv.org/abs/2203.11355>. arXiv:2203.11355 [cond-mat, stat].
- J. Lettvin, H. Maturana, W. McCulloch, and W. Pitts. What the Frog’s Eye Tells the Frog’s Brain. *Proceedings of the IRE*, 47(11):1940–1951, November 1959. ISSN 0096-8390. doi: 10.1109/JRPROC.1959.287207. URL <http://ieeexplore.ieee.org/document/4065609/>.
- Valerio Mante, David Sussillo, Krishna V. Shenoy, and William T. Newsome. Context-dependent computation by recurrent dynamics in prefrontal cortex. *Nature*, 503(7474):78–84, November 2013. ISSN 0028-0836, 1476-4687. doi: 10.1038/nature12742. URL <http://www.nature.com/articles/nature12742>.
- Vinod Nair and Geoffrey E. Hinton. Rectified linear units improve restricted boltzmann machines. In *Proceedings of the 27th international conference on international conference on machine learning*, ICML’10, pages 807–814, Madison, WI, USA, 2010. Omnipress. ISBN 978-1-60558-907-7. Number of pages: 8 Place: Haifa, Israel.
- Anh Nguyen, Jason Yosinski, and Jeff Clune. Multifaceted Feature Visualization: Uncovering the Different Types of Features Learned By Each Neuron in Deep Neural Networks, May 2016. URL <http://arxiv.org/abs/1602.03616>. arXiv:1602.03616 [cs].
- Roman Novak, Yasaman Bahri, Daniel A. Abolafia, Jeffrey Pennington, and Jascha Sohl-Dickstein. Sensitivity and Generalization in Neural Networks: an Empirical Study, June 2018. URL <http://arxiv.org/abs/1802.08760>. arXiv:1802.08760 [cs, stat].
- Chris Olah, Alexander Mordvintsev, and Ludwig Schubert. Feature visualization. *Distill*, 2017. doi: 10.23915/distill.00007.
- Chris Olah, Arvind Satyanarayan, Ian Johnson, Shan Carter, Ludwig Schubert, Katherine Ye, and Alexander Mordvintsev. The building blocks of interpretability. *Distill*, 2018. doi: 10.23915/distill.00010.
- Razvan Pascanu, Guido Montufar, and Yoshua Bengio. On the number of response regions of deep feed forward networks with piece-wise linear activations, February 2014. URL <http://arxiv.org/abs/1312.6098>. arXiv:1312.6098 [cs].
- Rodrigo Quian Quiroga, L. Reddy, G. Kreiman, C. Koch, and I. Fried. Invariant visual representation by single neurons in the human brain. *Nature*, 435(7045):1102–1107, June 2005. ISSN 0028-0836, 1476-4687. doi: 10.1038/nature03687. URL <http://www.nature.com/articles/nature03687>.

- Rodrigo Quian Quiroga, Alexander Kraskov, Christof Koch, and Itzhak Fried. Explicit Encoding of Multimodal Percepts by Single Neurons in the Human Brain. *Current Biology*, 19(15):1308–1313, August 2009. ISSN 09609822. doi: 10.1016/j.cub.2009.06.060. URL <https://linkinghub.elsevier.com/retrieve/pii/S0960982209013773>.
- Mattia Rigotti, Omri Barak, Melissa R. Warden, Xiao-Jing Wang, Nathaniel D. Daw, Earl K. Miller, and Stefano Fusi. The importance of mixed selectivity in complex cognitive tasks. *Nature*, 497(7451):585–590, May 2013. ISSN 0028-0836, 1476-4687. doi: 10.1038/nature12160. URL <http://www.nature.com/articles/nature12160>.
- David Rolnick and Konrad Kording. Reverse-engineering deep ReLU networks. In Hal Daumé III and Aarti Singh, editors, *Proceedings of the 37th international conference on machine learning*, volume 119 of *Proceedings of machine learning research*, pages 8178–8187. PMLR, July 2020. URL <https://proceedings.mlr.press/v119/rolnick20a.html>. tex.pdf: <http://proceedings.mlr.press/v119/rolnick20a/rolnick20a.pdf>.
- Shreya Saxena and John P Cunningham. Towards the neural population doctrine. *Current Opinion in Neurobiology*, 55:103–111, April 2019a. ISSN 09594388. doi: 10.1016/j.conb.2019.02.002. URL <https://linkinghub.elsevier.com/retrieve/pii/S0959438818300990>.
- Shreya Saxena and John P Cunningham. Towards the neural population doctrine. *Current Opinion in Neurobiology*, 55:103–111, April 2019b. ISSN 09594388. doi: 10.1016/j.conb.2019.02.002. URL <https://linkinghub.elsevier.com/retrieve/pii/S0959438818300990>.
- Justine Sergent, Shinsuke Ohta, and Brennan Macdonald. Functional neuroanatomy of face and object processing. A positron emission tomography study. *Brain*, 115(1):15–36, 1992. ISSN 0006-8950, 1460-2156. doi: 10.1093/brain/115.1.15. URL <https://academic.oup.com/brain/article-lookup/doi/10.1093/brain/115.1.15>.
- Rupesh Kumar Srivastava, Jonathan Masci, Faustino Gomez, and Jürgen Schmidhuber. Understanding Locally Competitive Networks, April 2015. URL <http://arxiv.org/abs/1410.1165>. arXiv:1410.1165 [cs].
- Christian Szegedy, Wojciech Zaremba, Ilya Sutskever, Joan Bruna, Dumitru Erhan, Ian Goodfellow, and Rob Fergus. Intriguing properties of neural networks. 2014. URL <https://arxiv.org/abs/1312.6199v4>.
- Seiji Tanabe. Population codes in the visual cortex. *Neuroscience Research*, 76(3):101–105, July 2013. ISSN 01680102. doi: 10.1016/j.neures.2013.03.010. URL <https://linkinghub.elsevier.com/retrieve/pii/S0168010213000874>.
- Lloyd N. Trefethen. *Approximation Theory and Approximation Practice, Extended Edition*. Society for Industrial and Applied Mathematics, Philadelphia, PA, January 2019. ISBN 978-1-61197-593-2 978-1-61197-594-9. doi: 10.1137/1.9781611975949. URL <https://epubs.siam.org/doi/book/10.1137/1.9781611975949>.
- Shaojie Xu, Joel Vaughan, Jie Chen, Aijun Zhang, and Agus Sudjianto. Traversing the local polytopes of ReLU neural networks. In *The AAAI-22 workshop on adversarial machine learning and beyond*, 2022. URL <https://openreview.net/forum?id=EQjwT2-Vaba>.
- Rafael Yuste. From the neuron doctrine to neural networks. *Nature Reviews Neuroscience*, 16(8):487–497, August 2015. ISSN 1471-003X, 1471-0048. doi: 10.1038/nrn3962. URL <http://www.nature.com/articles/nrn3962>.
- Bolei Zhou, Aditya Khosla, Agata Lapedriza, Aude Oliva, and Antonio Torralba. Object Detectors Emerge in Deep Scene CNNs. 2015. URL <https://arxiv.org/abs/1412.6856v2>.

A Polytope density while interpolating between activations caused by images

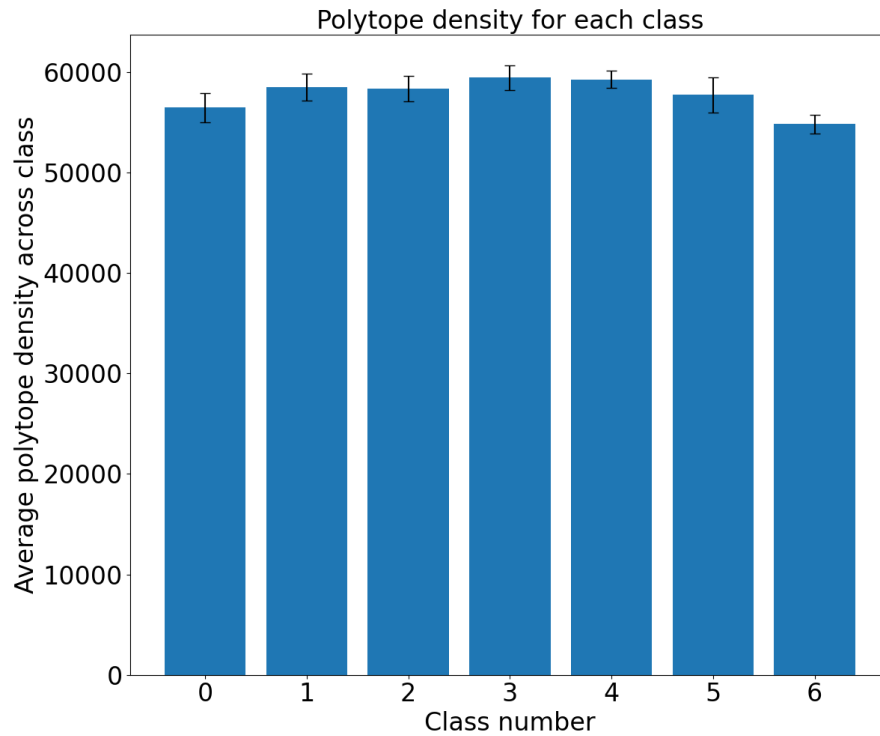


Figure 23: The polytope density for each class during a spherical interpolation between the activations caused by images of different classes in inception3a. The polytope codes were computed from the activations at layer 3a to the output layer. The polytope density was estimated by sampling 150 random points around each position during the interpolation and computing the number of polytopes passed through versus the euclidean distance. The interpolation path passes through multiple other classes. We see that the polytope density is highest in the intermediate region where there is much class change between intermediate classes. This trend is relatively weak, however. This provides tentative evidence in favor of the relationship between polytope density and semantic change in representation.

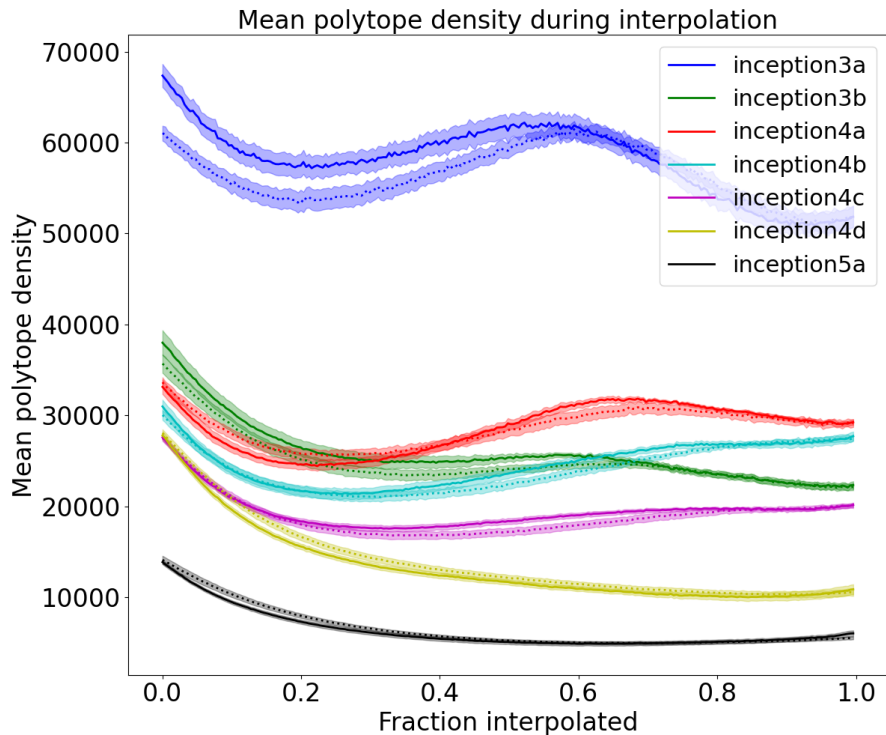


Figure 24: Mean polytope density (averaged over 200 image interpolations) by spherically interpolating between different class examples on each layer. Dotted lines represent the mean interpolation between images of the same class and solid lines represent the mean interpolation between images of different classes. The shaded regions represent the standard error of the mean. The polytope codes were computed from the embedding at the labeled layer to the output space. For lower imagenet layers, where the class labels are less informative of the semantic features, we see that the polytope density exhibits a double dip phenomenon where it increases when about half interpolated, indicating that interpolation leaves the manifold of typical activations. For later layers, the polytope density decreases and the curve flattens during interpolation implying that at these layers there are more monosemantic polytopes and the class labels are more representative of the feature distribution.

B Scaling activation vectors and plotting polytope density

Untrained network

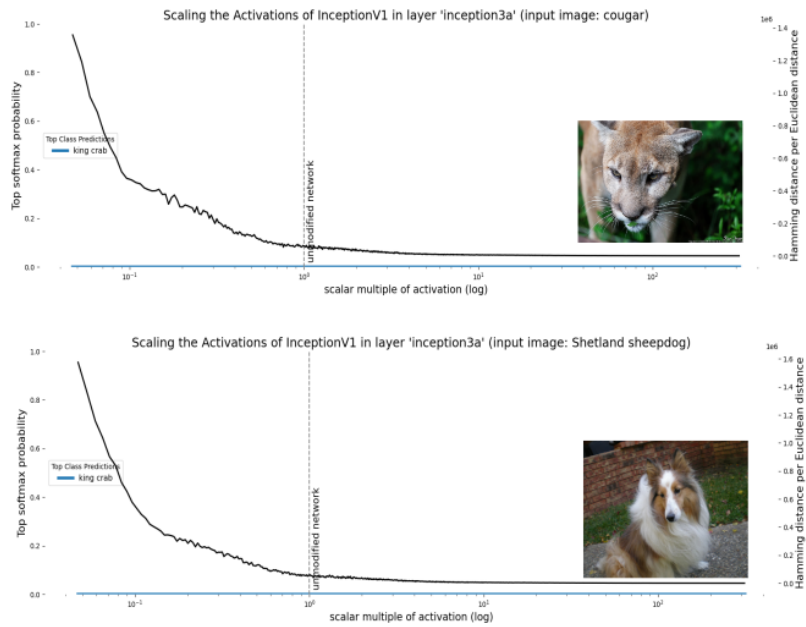


Figure 25: Note that the unchanging class in the untrained network is due to a phenomenon that resembles 'rank collapse': Even though the input and early activations are different, the activations of the untrained network converge on the same output. We believe this might be due to a quirk for our variant of InceptionV1 (perhaps its batchnorm), but we haven't investigated why exactly this happens.

With Gaussian noise activations

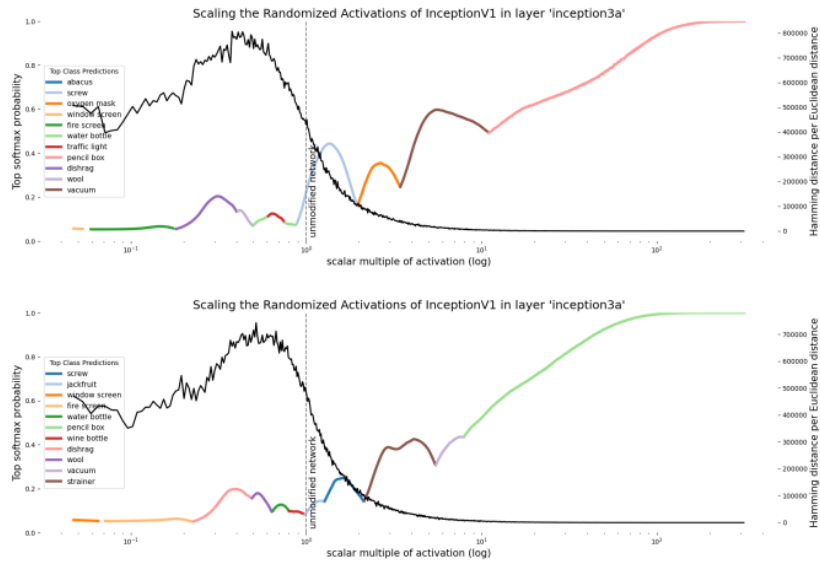


Figure 26

C Mathematical account of neural networks as max affine spline operators (MASOs)

In the below section we give an account of some recent theory from [Balestriero and baraniuk \(2018\)](#) that links deep neural networks to approximation theory via spline functions and operators. More specifically, the authors describe deep neural networks with piecewise linear activation functions (like ReLU) as compositions of *max-affine spline operators (MASOs)*, where each layer represents a single MASO. A MASO is an *operator* composed of a set of individual *max-affine spline* functions (MASs), one for each neuron in a given nonlinear layer.

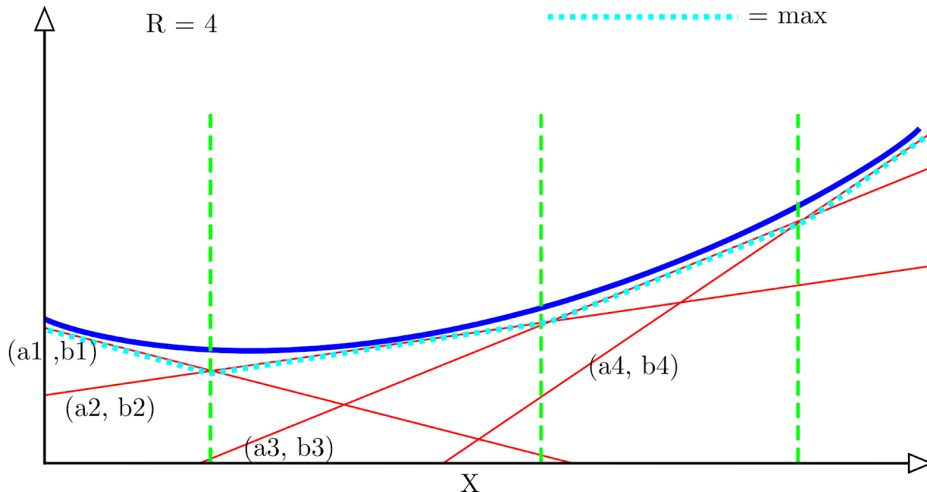
We won't go too deep into spline approximation theory here, but you can think of a spline function approximation in general as consisting of a set of partitions Ω^R of the input space, with a simple local mapping in each region. The *affine* part means that this mapping consists of an affine transformation of the input in a given region:

$$a_r x + b_r \text{ for } r = 1, \dots, R$$

The *max* part means that, instead of needing to specify the *partition region* of our input variable in order to determine the output, we can simply take the maximum value when we apply the entire set of affine transformations for each region:

$$z(x) = \max_{r=1, \dots, R} a_r x + b_r$$

A visual example is helpful to understand why this works. Suppose we have a spline approximation function with $R = 4$ regions:



Each red line represents a single spline with a corresponding affine transformation (a_r, b_r) , and the dotted light blue line represents the maximum value of all the affine transformations at each x location. We can see that it follows an approximation of the convex function (in dark blue).

A single ReLU unit can be expressed as a special case of *max-affine spline* with $R = 2$ regions:

$$\text{relu}(x) = \max_{r=1,2} a_r x + b_r$$

Where $(a_1, b_1) = (0, 0)$ and $(a_2, b_2) = (W_i, b_i)$, which are the weight and bias vectors for a given neuron. An entire ReLU layer can then be seen simply as a concatenation of d of these $R = 2$ MASs, where d is the width of the layer – this is our MASO.

This becomes slightly more complicated for smooth activation functions like GELU and Swish. But, fortunately, in a [later paper](#) the same authors extend their framework to just such functions. In summary - smooth activation functions must be represented with a *probabilistic* spline code rather than a one-hot binary code. The corresponding affine transformation at the input point is then a linear interpolation of the entire set of affine transformations, weighted by the input point's probability of belonging to each region.

D Note on Terminology of Superposition, Interference, and Aliasing

The concepts referred to by the terms ‘superposition’ and ‘interference’ [Elhage et al. \(2022\)](#) have parallel names in other literature. We provide this footnote with the hope of inspiring links between mechanistic interpretability and related results in signal processing, systems theory, approximation theory, physics, and other fields.

The [superposition principle](#) in the theory of linear systems refers to the fact that states of or solutions to a linear system may be added together to yield another state or solution. For example, solutions to linear wave equations may be summed to yield another solution. In this sense, superposition tells us that we can mathematically deduce the action of a system on any input from its action on a set of orthogonal basis vectors. This usage clashes with its usage in the mechanistic interpretability literature so far, where it has often been used to refer to systems without such a decomposition property. ‘Interference’ generally refers to superposition applied to linear waves. Specifically, the components of two waves interfere with each other, but orthogonal components within a wave do not.

The notion of ‘superposition’ and ‘interference’ as used in [Elhage et al. \(2022\)](#), where different features fail to be completely independent and inhibit correct measurements is similar to the idea of [aliasing](#) in other literatures. The term ‘aliasing’ originates in signal processing. In that context, aliasing arose from the indistinguishability of waves of different frequencies under discrete sampling schemes. Aliasing has come to refer more generally to the phenomenon in which a set of desired quantities (e.g. features) fails to be orthogonal with respect to a measurement basis. If we wish to determine the value of n features from $k \ll n$ measurements, some sets of feature values may yield the same measurements. In the case of sampling waves, high-frequency waves may appear the same as low-frequency waves. In the case of approximating functions from k many sample points, high-degree polynomials may take the same values on those k points (see [Trefethen, 2019](#), Chapter 4 for a discussion in the case of Chebyshev interpolation). In image processing, [anti-aliasing](#) is used to deal with visual artifacts that come from high-frequency components being indistinguishable from lower frequency components.

Quantum mechanics uses the conventions we have described. A quantum system with two possible classical states $|0\rangle$ and $|1\rangle$ has its quantum state described as an orthogonal superposition of the form $a|0\rangle + b|1\rangle$ where a and b are complex numbers. The two classical states do not ‘interfere’ with each other. Rather, two independent quantum systems may additively interfere with corresponding orthogonal components interfering. Interference and superposition in this context are not referring to entanglement. Just as we may represent $(|0\rangle + |1\rangle)/\sqrt{2}$ as a superposition of the states $|0\rangle$ and $|1\rangle$, we may also represent the state $|0\rangle$ as a superposition of the states $(|0\rangle + |1\rangle)/\sqrt{2}$ and $(|0\rangle - |1\rangle)/\sqrt{2}$. The important detail regarding ‘superposition’ is the additivity, not the particular choice of classical states for our representation. The [quantum harmonic oscillator](#) has eigenstates (orthogonal basis vectors for the system) described by [Hermite polynomials](#). If we approximate the Hermite polynomials with an asymptotic approximation, we will observe aliasing due to the failure of our approximation to be perfectly orthogonal.

Model: GPT2-small Layer: (9, 10, 11) Cluster ID: 197

<p>CR47]). Due to the limited diversity of *Pf*AMA-1 antigens, vaccines targeting a small number of *Pf*AMA-1 alleles might be sufficient to cover naturally circulating populations of *P. falciparum* in different endemic areas \[@CR33]. These results also indicate that the global genetic diversity of *Pf*AMA-1 is relatively limited, even though substantial geographic differentiation can also be identified among populations. Nevertheless, global *Pf*AMA-1 is undergoing natural selection and high levels of meiotic recombination, which can produce new alleles in a gene population. Therefore, consideration should be given to the development of *Pf*AMA-1-based malaria vaccines using a polyallelic approach to maximize vaccine effectiveness. To assess the association between host immune pressure and natural selection of *Pf*AMA-1, genetic polymorphisms in predicted B-cell epitopes and I</p>
<p>damages suffered by the "defendants" and that the court took no action and made no decision regarding the cross-complaint. Section 581d of the Code of Civil Procedure provides that the dismissal of an action by the court shall be entered upon the minutes and upon the clerk's register, and that when entered upon the minutes it shall constitute a judgment and be effective for all purposes. The order of dismissal was entered upon the minutes of the court and upon the clerk's register of actions and therefore, constituted a final judgment. The *853 order of August 26 vacating the order of dismissal was a special order made after final judgment and appealable under the provisions of section 963, subdivision 2, of the Code of Civil Procedure. Nicholson v. Henderson, 25 Cal.2d 375 [153 P.2d 945], and Krug v. Mechan, 106 Cal.App.2d 554 [235 P.2d 410], relied upon by the plaintiff</p>
<p>-09-00094} ----- Obviously, the host is also a very important element in the development of the disease, which is influenced by fish species, fish age, physiological conditions, and even the genetic characteristics of the individuals. It is well known that the species most susceptible to IPN disease are salmonids, mainly rainbow trout and Atlantic salmon \[@B4-pathogens-09-00094], in which the virus produces the most frequent and characteristic symptoms. However, as already described above, IPNV has been isolated from diseased fish from other species such as European and Japanese eels (*Anguilla anguilla* and *A. japonica*, respectively), in which it produces necrosis of the gill lamellar cells, yellowtail (*Seriola quinqueradiata*), where the virus is known as the yellowtail ascites virus, and flatfish such as turbot (*Scophthalmus maximus*) and</p>
<p>to cure requirements, demonstrates the parties' intent to dispense these requirements under certain Events of Default. Thus, the nature of the premises is not necessarily a basis for concluding that the Lease requires notice and opportunity to cure for nonpayment of rent. For all the reasons discussed above, we conclude that the trial court erred in finding that subparagraph 10.1.9 requires Landlords to provide notice of default to USH and an opportunity to cure as to the nonpayment of rent. That said, we must address Hoosier's argument that Landlords were required to provide notice to USH and an opportunity to cure pursuant to Indiana common law principles, and therefore the trial court did not err in ruling that Landlords' complaint was premature and did not terminate the Lease.[11] In support of its argument, Hoosier relies on Scott-Reitz Ltd. v. Rein Warsaw Associates, 658 N.E.2d 98 (Ind.Ct.App.1995</p>

Figure 29: A cluster responding to words followed by commas (or conjunctive pronouns?).

Model: GPT2-small Layer: (7, 8, 9, 10, 11) Cluster ID: 31

<p>in schools. They added signage in the Berber script, Tamazight, to government buildings. Cultural rights defused some of the anger, but the protests were sustained by economic marginalisation and when they continued the authorities often responded with force. Kurdish aspirations offered a greater prospect of realisation. Western powers had first promised the Kurds a state when they carved up the Ottoman Empire in the Treaty of Sevres in 1920, but changed their minds with the Treaty of Lausanne three years later. The unravelling of Iraq gave Kurds a fresh chance. Western powers had financed and supported Kurdish capacity-building since the 1991 Gulf War when they established a no-fly zone over a Kurdish safe-haven. Each national crisis gave Kurds greater leverage. Iraq's 2005 constitution made Kurdish one of Iraq's two official languages and upgraded the autonomous enclave into a Kurdistan Regional Government (KRG) with its own US-</p>
<p>They kept an even pace, Michael allowing her to take the lead through narrow switch backs. Kris's mind continued to wander. Adam was a talker. Talk, talk, talk. Boasting about all his exclusive knowledge, expertise, abilities. It had become so intrusive to Kris that she found herself screaming at him to shut the fuck up on a regular basis. A large crack in her usual quiet behavior demonstrated the severity of problems and ultimately led to the break up months ago. Six months gone by. Adam wasn't giving up on the hope they'd be back together as a couple some day. Kris was aware, he'd been messing around with other females. Rumors pass quickly in a small community, and she'd received an ear full of his sexual promiscuity. Sex was highly important to him. His only way of mistakenly believing he had achieved the ultimate bond with a female. The sun reached the high point in the sky casting an intense glare off the granite</p>
<p>, some more nuanced than others...But the synopsis is it regulates carrier velocity, changes felt recoil impulse, and most importantly, it opens up the entire operational envelope of the gun. It allows the gun to run properly under a much wider range of input and factors. This usually equates to more overall reliability...which is a good thing. Q: Let ◆◆ start at the beginning, how did the VLTOR A5 Buffer System come about? Nick Wantland: Years ago, the Marine Corps was looking at ways to deal with the ergonomic and length-of-pull issues they were having with the fixed stocks on their M16A4s. The fixed stock was designed long ago before the introduction of thick, modern body armor. Depending on the Marine ◆◆ body type, and what style optic they were using, the lack of adjustability in the stock length was causing tons of ergonomic, mobility, and eye relief issues. To compensate</p>
<p>at her trembling hands, tears welling not from joy or consternation or even sadness but some vague and growing dread. She wiped her dampened eyes on the sleeve of Matthew's shirt. Press ahead, she advised herself. The idea will protect you from the part of yourself that should always have been restrained from hurting others. The sun was strong through the windows and cast a checkerboard of shadows on the counter, the floor, the table, her hands, the list. Three years</p>

Figure 30: A cluster responding to spans of time.

Activation clusters:

Model: GPT2-small Layer: 0 Cluster ID: 777

? "We're so precious, aren't we?" "Everyone has got to live." "Everyone has got to be happy." "It's a joke." "It's an absolute joke." "Humanity can't survive over the next 100 years." "The facts don't lie." "We need someone who will stand for something." "We need someone who believes in what they say and believes in action, believes in positive action." "It's an absolute joke." "Evan, that's what you didn't get." "That's what you didn't get." "You think people are equal." "They're not." "They're not." "¶" "{Newscasters overlapping}...just like President Richard Nixon did to the Vietnamese back in the late '60s" "Osama bin Laden, al Qaeda, these people are out to kill us." "People don't" "All of these things contribute to the problem of overpopulation." "People don't comprehend

, that's for sure. A regular little fireball, you are. I love it! Hah, hah, hah! You're so cute when you're mad. (_Again he leans back on the bedding, his head hanging down, and throws out his legs. Belying his words, he shakes his legs as if to fan the flames of agony in his heart._) OK (_Sharply_): I told you, get out!... This is the Inaba House, Oko's place. No, it belongs to Mr. Katsuragi. It's his...second residence. DENGU: I don't give a damn if it's a whorehouse. If I'm in the way, I'll just crawl into the closet. Hah, hah, hah! (_Laughs mirthlessly_) OK: What's the point of losing my temper? You're a cockroach,

." "we take the bus all year long, we never eat out, we share deodorant." "this is the one thing that we do right all year long and now we can't even have that, so what does that make us?" "well, we still got each other." "fuck that shit." "they, walter, what's up?" "oh, hey." "got an extra smoke?" "oh, i'm sorry, this is my last one." "that's all right." "oh, man, what a day." "yeah." "did you have to work today?" "yup." "on a holiday?" "that sucks." "4th of july is the worst." "man, they don't pay me enough for this shit." "yeah, i know, all right?" "you don't know." "what do you mean?" "we have trouble paying our bills." "i know how you feel." "no, you

." "we take the bus all year long, we never eat out, we share deodorant." "this is the one thing that we do right all year long and now we can't even have that, so what does that make us?" "well, we still got each other." "fuck that shit." "they, walter, what's up?" "oh, hey." "got an extra smoke?" "oh, i'm sorry, this is my last one." "that's all right." "oh, man, what a day." "yeah." "did you have to work today?" "yup." "on a holiday?" "that sucks." "4th of july is the worst." "man, they don't pay me enough for this shit." "yeah, i know, all right?" "you don't know." "what do you mean?" "we have trouble paying our bills." "i know how you feel." "no, you

." "we take the bus all year long, we never eat out, we share deodorant." "this is the one thing that we do right all year long and now we can't even have that, so what does that make us?" "well, we still got each other." "fuck that shit." "they, walter, what's up?" "oh, hey." "got an extra smoke?" "oh, i'm sorry, this is my last one." "that's all right." "oh, man, what a day." "yeah." "did you have to work today?" "yup." "on a holiday?" "that sucks." "4th of july is the worst." "man, they don't pay me enough for this shit." "yeah, i know, all right?" "you don't know." "what do you mean?" "we have trouble paying our bills." "i know how you feel." "no, you

Figure 31: A 'detokenization' cluster that responds both to the word "is" and its contraction.

Model: GPT2-small Layer: 4 Cluster ID: 673

[*et al.*]{} \{BaBar Collaboration\}, Phys. Rev. D [**84**]{} , 092003 (2011) \[arXiv:1108.5874 \[hep-ex\]\]. U. Tamponi [*et al.*]{} \{Belle Collaboration\}, Phys. Rev. Lett. [**115**]{} , no. 14, 142001 (2015) \[arXiv:1506.08914 \[hep-ex\]\]. Y. P. Kuang, Front. Phys. China [**1**]{} , 19 (2006) \[hep-ph/0601044\]. M. B. Voloshin, Prog. Part. Nucl. Phys. [**61**]{} , 455 (2008) \[ar

three dimensions, Mod. Phys. A [**8**]{} (1993) 3371. P. S. Howe, J. M. Izquierdo, G. Papadopoulos and P. K. Townsend, New supergravities with central charges and Killing spinors in (2+1)-dimensions, Nucl. Phys. B [**467**]{} (1996) 183 \[hep-th/9505032\]. M. Banados, R. Troncoso and J. Zanelli, Higher dimensional Chern-Simons supergravity, Phys. Rev. D [**54**]{} (1996) 2605 \[gr-qc/9601003\]. A. Giacomini, R. Troncoso and

in the _Labour Leader_ , 20 April 1901. . _Dewsbury Reporter_ , 13 October 1894. . _Tom Maguire, a Remembrance_ , p. vi. Snowden, _op. cit._ , p. 82. . _Tom Maguire, a Remembrance_ ; T. Maguire, _Machine Room Chants_ (1895); J. Clayton, _Before Sunrise_ (Manchester, 1896); miscellaneous cuttings in Turner and Mattison Scrapbooks, and Mattison Notebook. ## _Index_ The index that appeared in the print version of this title was intentionally removed from the eBook. Please use the search function on your eReading device for terms of interest. For your reference, the terms that appear in the print index are listed below Abel-Smith, Brian affluence "Against University Standards" (Thompson)

1119–1152. T. M. Smith, R. W. Reynolds, R. E. Livezey, and D. C. Stokes, Reconstruction of historical sea surface temperatures using empirical orthogonal functions, J. Clim. 9 (1996) 1403–1420. M. Newman, G. F. Compo, and M. A. Alexander, ENSO-forced variability of the pacific decadal oscillation, J. Clim. 16 (2003) 3853–3957. P. U. Clark, N. G. Piasias, T. F. Stocker, and A. J. Weaver, The role of the thermohaline circulation in abrupt climate change, Nature 415 (2002) 863–869. R. Bracewell, The Fourier Transform and Its Applications, McGraw-Hill (1999). S. Kak, The discrete Hilbert transform, Proc. IEEE 58 (1970), 585-

-Doo! in Where's My Mummy? (May 2005) Noddy Saves Christmas (December 2005) My Little Pony: The Princess Promenade (January 2006) Roach Approach: Slingshot Slugger (February 2006) Pinocchio 3000 (April 2006) The Secret of the Sword (May 2006) Arthur's Missing Pal (July 2006) My Little Pony: The Runaway Rainbow (August 2006) Holly Day (September, 2006) Strawberry Shortcake: The Sweet Dreams Movie (October 2006) A Christmas Carol (December 2006) My Little Pony: A Very Pony Place (January 2007, August 2009) The Little Robots in the Big Show (February 2007) Strawberry Shortcake: Berry Blossom Festival (March 2007) Jakers!: Wish Upon a Story (April 2007) Eloise in Hollywood (May 2007) Holly Hobbie & Friends: Best Friends Forever

Figure 32: A cluster responding to dates.

